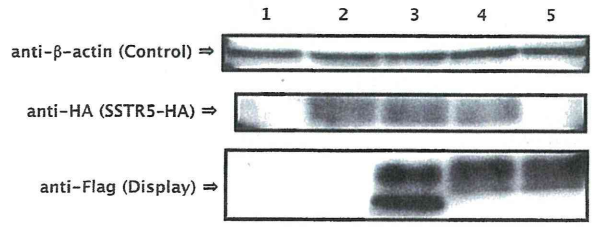

Figure 5. Confirmation of protein expression. Western blots of extracts from somatostatin displaying yeast strains. Lane 1: Mock/Mock, 2: SSTR5/Mock, 3: SSTR5/Flag–Flo42, 4: SSTR5/S-14–Flag–Flo42, 5: Mock/S-14–Flag–Flo42. Anti-β-actin antibody was used as loading control. Anti-HA antibody was used for detection of SSTR5 receptor. Anti-Flag antibody was used for detection of Flag–Flo42 anchor or S-14–Flag–Flo42 fusion proteins. IMFD-70 was used as the host strain. The transformants used in these experiments are listed in Table S3.
doi:10.1371/journal.pone.0037136.g005

Yeast Strains

Yeast strains used for assays were generated from BY4741 [31] as a parental backbone strain and are listed in Table 1. The transformation procedure using linear DNA fragments followed the lithium acetate method [32]. All primers used for the strain constructions are listed in Table S1. The *bar1*Δ alleles that relieve the degradation of α-factor pheromone [33] were conferred to BY4741*far1*Δ (obtained from *Saccharomyces* Genome Deletion Project [34]) by homologous recombination with the amplified *LEU2* fragments, producing the IM-4 strain. The *FUS1-GFP* reporter gene was integrated into the *FUS1* genomic loci of IM-4 with a fragment prepared by digestion of pUC119-FUS1-EGFP-HIS3 [28] with EcoRI and SphI, producing the IMG-4 strain. The P_{FUS1}-*FUS1-GFP* or P_{FIG1}-*GFP* reporter gene was used to monitor signal transduction promoted by stimulating GPCRs in yeast (IMG-4, IMG-50 or IMFD-70 [5]). *far1*Δ alleles were used to avoid G1 arrest and promote cell-cycle progression during signal activation [5,28,35] (IMG-4 and IMFD-70). *sst2*Δ and *ste2*Δ alleles were used to obtain hypersensitivity for ligand stimulation and to inhibit competitive expression of endogenous yeast GPCRs [5,28] (IMG-50 and IMFD-70).

Plasmids

All plasmids used for assays are listed in Table 1. All primers used for plasmid constructions are listed in Table S1. The amplified pre, pro (containing secretion signal sequence, s.s.) and first mature sequences of α-factor peptide including a C-terminal Flag tag and stop codon were inserted into the pESC-URA yeast expression vector (Agilent Technologies, Santa Clara, CA, USA) at the BamHI and XhoI sites, creating pUESCαsf. As the backbone for α-factor-displaying plasmids, pUESCαf and pUESCαf(AG) without stop codons were constructed in essentially the same manner. The amplified genes encoding Flo42, Flo102, Flo146 and Flo318 anchors were inserted into pUESCαf at the XhoI and NheI sites, resulting in pUESCαf-FLO42, -FLO102, -FLO146 and -FLO318, respectively. pUESCαf-AG was produced in a similar procedure by inserting the gene encoding the C-terminal 320 aa of Sag1p (C-terminal half of α-agglutinin anchor, AG) into pUESCαf(AG) at the XhoI and NheI sites. As the backbone for somatostatin-displaying plasmids, we constructed pGK426-tgFLO42 by inserting the amplified *FLO42* anchor gene with *FLAG* at the N-terminus into pGK426 at the SalI and BglII sites [36]. The DNA fragment containing s.s. of α-factor and S-14 mature peptide was amplified by overlapping PCR and inserted into pGK426-tgFLO42 at the NheI and SalI sites, producing pGK-S1442. We generated pGK-alpha42 as an α-factor peptide-displaying control plasmid, using essentially the same procedure. As other peptide-displaying control plasmids, the gene containing s.s. of α-factor and the mature peptide sequences of angiotensin II (AII) or endothelin-1 (ET1) was inserted into pGK426-tgFLO42 at the NheI and SalI sites, generating pGK-AII42 and pGK-ET142, respectively. As a peptide-non-displaying control plasmid, pGK42 was created in a similar procedure by using the DNA fragment containing s.s. of α-factor without the peptide sequence. pGK-SSTR5-HA [5,6] was used to express human SSTR5 receptor fused to a C-terminal HA tag. Transformation of plasmids was performed using the lithium acetate method. All transformants used for assays are listed in Table S3.

Pheromone Signaling Assay

To assay signal activation from the endogenous Ste2 pheromone receptor, the IMG-4 yeast strains harboring the

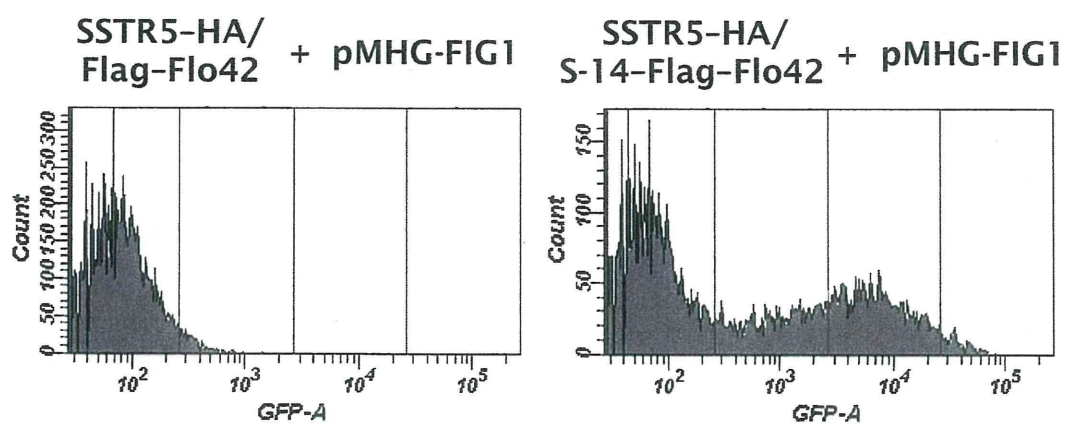

Figure 6. Improved fluorescence signal in the CWTrAP system using somatostatin peptide for the human SSTR5 receptor. SSTR5 signaling assays of the cyclic somatostatin peptide displaying yeast strain and the non-displaying control strain, which contain the multi-copy plasmid harboring a *GFP* reporter gene cassette (pMHG-FIG1). IMFD-70 was used as the host strain. The transformants used in these experiments are listed in Table S3.
doi:10.1371/journal.pone.0037136.g006

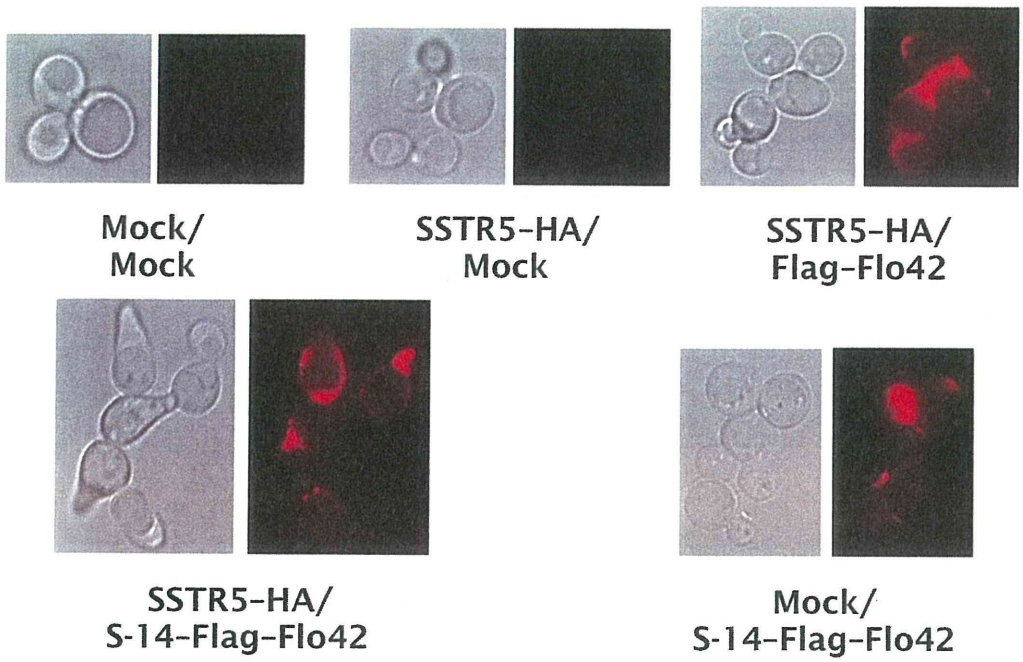

Figure 7. Confirmation of peptide trapping on yeast cell surfaces. Immunofluorescence staining of somatostatin displaying yeast strains. Anti-Flag antibody and Alexa Fluor 594-conjugating secondary antibody were used for detection of Flag–Flo42 anchor or S-14–Flag–Flo42 fusion proteins. Red fluorescence images are shown in false-color. IMFD-70 was used as the host strain. The transformants used in these experiments are listed in Table S3.
doi:10.1371/journal.pone.0037136.g007

pESC-URA-based plasmids were grown in SR media at 30°C, and cells were then inoculated into 100 ml of SRGC media to give an initial optical density of 0.03 at 600 nm. Cultures were grown at 30°C with shaking at 150 opm for 72 h. The cells were collected and diluted into test tubes containing sheath solution and GFP fluorescence was measured using a BD FACSCalibur flow cytometer (BD Biosciences, San Jose, CA, USA). The green fluorescence signal from 10,000 cells was excited with an argon laser and collected through a 530/30 nm band-pass (FL1) filter. The data were analyzed using BD CELLQuest software (BD Biosciences). The "relative fluorescence unit" was defined using the FL1-H geometric mean of IMG-4 harboring mock plasmid (pESC-URA) as the benchmark.

SSTR5 Signaling Assay

To assay signal activation from human SSTR5 receptor, the IMFD-70 yeast strains harboring the pGK-SSTR5-HA and pGK426-based plasmids were grown in SD media at 30°C, and cells were then inoculated into 20 ml of SDM71 media to give an initial OD_{600} of 0.03. Cultures were grown at 30°C with shaking at 150 opm for 15 h. The cells were collected and diluted into test tubes containing sheath solution and GFP fluorescence was measured using a BD FACSCanto II flow cytometer (BD Biosciences). The green fluorescence signal from 10,000 cells was excited with a blue laser and collected through a 530/30 nm band-pass (GFP) filter. The data were analyzed using BD FACSDiva software (BD Biosciences).

Western Blotting

Collected cells were suspended in 10 mM Tris-HCl (pH 7.8) containing 1 mM phenylmethylsulfonyl fluoride (PMSF) to give an OD_{600} of 5, and 200 µl of cell suspension was disrupted using a Multi-beads shocker (Yasui Kikai, Osaka, Japan) with 0.5 mm glass beads. Cell lysates were centrifuged at 1,000×g for 5 min and the pellet was then washed three times with 10 mM Tris-HCl containing 1 mM PMSF. The pellet was resuspended in 200 µl of SDS solubilization buffer (50 mM Tris-HCl [pH 7.8], 2% SDS [w/v], 100 mM ethylene diamine tetraacetic acid [EDTA], 40 mM 2-mercaptoethanol [2-ME]), and the suspension was boiled at 95°C for 5 min and then centrifuged at 10,000×g for 5 min. The supernatant was collected and diluted with an equivalent volume of 2× sample buffer (25 mM Tris-HCl [pH 6.8], 4% SDS [w/v], 20% glycerol [w/v], 10% 2-ME [v/v], 0.1 mg/ml bromophenol blue [BPB]). Twenty microliters of each sample was loaded onto a 12.5% SDS-polyacrylamide gel and proteins were separated by electrophoresis and then transferred to polyvinylidene fluoride (PVDF) membrane (Immobilon-FL; Millipore, Billerica, MA, USA) by electroblotting. Western blots were performed as follows: mouse anti-β-actin monoclonal antibody (Abcam, Cambridge, UK) as loading control, rabbit anti-HA antibody (Bethyl Laboratories, Montgomery, TX, USA) for HA-tagged SSTR5 receptor, and mouse anti-Flag M2 monoclonal antibody (Sigma-Aldrich, St. Louis, MO, USA) for fusion proteins with S-14 peptide, Flag tag and Flo42 anchors were primarily used at dilutions of 1:5,000 in TBST (10 mM Tris-HCl [pH 8.0], 150 mM NaCl, 0.05% Tween-20 [v/v]). Anti-mouse or anti-rabbit secondary antibodies conjugated with alkaline phosphatase (Promega, Madison, WI, USA) were used at dilutions of 1:5,000 in TBST. Chemiluminescent visualization was performed with Amersham CDP-Star Detection Reagent (GE Healthcare, Buckinghamshire, UK) and the signal was detected using a lumino-image analyzer LAS-1000mini system (Fujifilm, Tokyo, Japan).

Immunofluorescent Staining

For α-factor displaying yeasts (IMG-4), collected cells were diluted to give an $OD_{600} = 10$ with distilled water and the cell suspension was used for immunofluorescence staining by incubating with mouse anti-Flag M2 monoclonal antibody (Sigma-Aldrich) at a dilution of 1:500 for 1 h at room temperature. After washing in triplicate, anti-mouse secondary antibody conjugated with Alexa Fluor 546 (Invitrogen Life Technologies, Carlsbad, CA, USA) at a dilution of 1:500 was incubated with the cell suspensions for 1 h at room temperature. After washing in triplicate, cells were resuspended in distilled water and observed on a fluorescence microscope with a monochrome CCD camera. To obtain micrographs of better clarity, essentially the same procedure was used for somatostatin displaying yeasts (IMFD-70), but the density of the collected cells was adjusted to $OD_{600} = 5$. Antibodies were used at a dilution factor of 1:100. Anti-mouse IgG conjugated with Alexa Fluor 594 (Invitrogen Life Technologies) was used as the secondary antibody.

Supporting Information

Figure S1 Western blotting of SDS-extracted fractions from the IMG-4/pUESCαf-FLO42 yeast strain. $EndoH_f$ (Endoglycosidase H) was used to confirm glycosylation of the Flo42 anchor. Anti-Flag M2 monoclonal antibody and anti-mouse secondary antibody conjugated with alkaline phosphatase were used to detect the α-factor Flag Flo42 fusion protein. NBT (nitro blue tetrazolium) and BCIP (5-bromo-4-chloro-3-indolyl-phosphate) were used for the colorimetric reaction.
(TIF)

Figure S2 Pheromone signaling assays of α-factor-displaying yeast strains with various anchor motifs (color histograms). Gray histograms show the data from control strains (mock). IMG-4 was used as the host strain. The transformants used in this experiment are listed in Table S3.
(TIF)

Figure S3 SSTR5 signaling assays of somatostatin-displaying yeast strains with various secretion signal sequences (color histograms). The Flo42 anchor was used for somatostatin display. S-28 indicates the 28 aa active isoform of somatostatin peptide. Gray histograms show the data from control strains (mock). Cultures were grown in SDM71 media for 22 h. IMG-50 was used as the host strain. The transformants used in this experiment are listed in Table S3.
(TIF)

Figure S4 SSTR5 signaling assays of somatostatin-displaying yeast strains with different length GS linkers (color histograms). The S-14 peptide and Flo42 anchor were used for display. Gray histograms show the data from control strains (mock). Cultures were grown in SDM71 media for 12 h. IMG-50 was used as the host strain. The transformants used in this experiment are listed in Table S3.
(TIF)

Figure S5 SSTR5 signaling assays of somatostatin-displaying yeast strain (target cells) mixed with somatostatin-non-displaying strain (non-target cells). S-14 Flag Flo42 and Flag Flo42 fusion proteins were used as target and non-target cells, respectively. R1 regions in the dot plots show the gates for FACS sorting. The ratio of initial cell densities was adjusted to 10:1 (non-target cells : target cells), and the cultures were grown in SDM71 media. IMG-50 was used as the host strain. The transformants used in this experiment are listed in Table S3.
(TIF)

Table S1 List of primers.
(PDF)

Table S2 Plasmids used in Supplementary data.
(PDF)

Table S3 List of strains and transformants used for assays.
(PDF)

Document S1 Supplementary Materials and Methods (Plasmid constructions for supporting information).
(PDF)

Acknowledgments

We thank Dr. Ikuo Fujii, Dr. Takeshi Tsumuraya (Osaka Prefecture University), and Dr. Mitsuyoshi Ueda (Kyoto University) for helpful discussion.

Author Contributions

Conceived and designed the experiments: JI NY KT SK CO HF AK. Performed the experiments: JI. Analyzed the data: JI. Contributed reagents/materials/analysis tools: JI. Wrote the paper: JI AK.

References

1. Rasmussen SG, Choi HJ, Rosenbaum DM, Kobilka TS, Thian FS, et al. (2007) Crystal structure of the human β2 adrenergic G-protein-coupled receptor. Nature 450: 383–387.
2. Vögler O, Barceló JM, Ribas C, Escribá PV (2008) Membrane interactions of G proteins and other related proteins. Biochim Biophys Acta 1778: 1640–1652.
3. Ishii J, Fukuda N, Tanaka T, Ogino C, Kondo A (2010) Protein-protein interactions and selection: yeast-based approaches that exploit guanine nucleotide-binding protein signaling. FEBS J 277: 1982–1995.
4. Heilker R, Wolff M, Tautermann CS, Bieler M (2009) G-protein-coupled receptor-focused drug discovery using a target class platform approach. Drug Discov Today 14: 231–240.
5. Togawa S, Ishii J, Ishikura A, Tanaka T, Ogino C, et al. (2010) Importance of asparagine residues at positions 13 and 26 on the amino-terminal domain of human somatostatin receptor subtype-5 in signalling. J Biochem 147: 867–873.
6. Iguchi Y, Ishii J, Nakayama H, Ishikura A, Izawa K, et al. (2010) Control of signalling properties of human somatostatin receptor subtype-5 by additional signal sequences on its amino-terminus in yeast. J Biochem 147: 875–884.
7. Fukuda N, Ishii J, Kaishima M, Kondo A (2011) Amplification of agonist stimulation of human G-protein-coupled receptor signaling in yeast. Anal Biochem 417: 182–187.
8. Ryo S, Ishii J, Iguchi Y, Fukuda N, Kondo A (2012) Transplantation of the GAL regulon into G-protein signaling circuitry in yeast. Anal Biochem 424: 27–31.
9. Li B, Scarselli M, Knudsen CD, Kim SK, Jacobson KA, et al. (2007) Rapid identification of functionally critical amino acids in a G protein-coupled receptor. Nat Methods 4: 169–174.
10. Baranski TJ, Herzmark P, Lichtarge O, Gerber BO, Trueheart J, et al. (1999) C5a receptor activation. Genetic identification of critical residues in four transmembrane helices. J Biol Chem 274: 15757–15765.
11. Ueda M, Tanaka A (2000) Genetic immobilization of proteins on the yeast cell surface. Biotechnol Adv 18: 121–140.
12. Kondo A, Ueda M (2004) Yeast cell-surface display-applications of molecular display. Appl Microbiol Biotechnol 64: 28–40.
13. Shibasaki S, Maeda H, Ueda M (2009) Molecular display technology using yeast-arming technology. Anal Sci 25: 41–49.
14. Gai SA, Wittrup KD (2007) Yeast surface display for protein engineering and characterization. Curr Opin Struct Biol 17: 467–473.
15. Pepper LR, Cho YK, Boder ET, Shusta EV (2008) A decade of yeast surface display technology: where are we now? Comb Chem High Throughput Screen 11: 127–134.
16. Murai T, Ueda M, Atomi H, Shibasaki Y, Kamasawa N, et al. (1997) Genetic immobilization of cellulase on the cell surface of Saccharomyces cerevisiae. Appl Microbiol Biotechnol 48: 499–503.

17. Sato N, Matsumoto T, Ueda M, Tanaka A, Fukuda H, et al. (2002) Long anchor using Flo1 protein enhances reactivity of cell surface-displayed glucoamylase to polymer substrates. Appl Microbiol Biotechnol 60: 469 474.
18. Matsumoto T, Fukuda H, Ueda M, Tanaka A, Kondo A (2002) Construction of yeast strains with high cell surface lipase activity by using novel display systems based on the Flo1p flocculation functional domain. Appl Environ Microbiol 68: 4517 4522.
19. Tanino T, Matsumoto T, Fukuda H, Kondo A (2004) Construction of system for localization of target protein in yeast periplasm using invertase. J Mol Catal, B Enzym 28: 259 264.
20. Nakamura Y, Shibasaki S, Ueda M, Tanaka A, Fukuda H, et al. (2001) Development of novel whole-cell immunoadsorbents by yeast surface display of the IgG-binding domain. Appl Microbiol Biotechnol 57: 500 505.
21. Antipov E, Cho AE, Wittrup KD, Klibanov AM (2008) Highly L and D enantioselective variants of horseradish peroxidase discovered by an ultrahigh-throughput selection method. Proc Natl Acad Sci USA 105: 17694 17699.
22. Feldhaus MJ, Siegel RW, Opresko LK, Coleman JR, Feldhaus JM, et al. (2003) Flow-cytometric isolation of human antibodies from a nonimmune Saccharomyces cerevisiae surface display library. Nat Biotechnol 21: 163 170.
23. Boder ET, Midelfort KS, Wittrup KD (2000) Directed evolution of antibody fragments with monovalent femtomolar antigen-binding affinity. Proc Natl Acad Sci USA 97: 10701 10705.
24. Nakayama N, Miyajima A, Arai K (1987) Common signal transduction system shared by STE2 and STE3 in haploid cells of Saccharomyces cerevisiae: autocrine cell-cycle arrest results from forced expression of STE2. EMBO J 6: 249 254.
25. Dolan JW, Kirkman C, Fields S (1989) The yeast STE12 protein binds to the DNA sequence mediating pheromone induction. Proc Natl Acad Sc. USA 86: 5703 5707.
26. Møller LN, Stidsen CE, Hartmann B, Holst JJ (2003) Somatostatin receptors. Biochim Biophys Acta 1616: 1 84.
27. Burgus R, Ling N, Butcher M, Guillemin R (1973) Primary structure of somatostatin, a hypothalamic peptide that inhibits the secretion of pituitary growth hormone. Proc Natl Acad Sci USA 70: 684 688.
28. Ishii J, Tanaka T, Matsumura S, Tatematsu K, Kuroda S, et al. (2008) Yeast-based fluorescence reporter assay of G protein-coupled receptor signalling for flow cytometric screening: FAR1-disruption recovers loss of episomal plasmid caused by signalling in yeast. J Biochem 143: 667 674.
29. Leberer E, Thomas DY, Whiteway M (1997) Pheromone signalling and polarized morphogenesis in yeast. Curr Opin Genet Dev 7: 59 66.
30. Müller S, Nebe-von-Caron G (2010) Functional single-cell analyses: flow cytometry and cell sorting of microbial populations and communities. FEMS Microbiol Rev 34: 554 587.
31. Brachmann CB, Davies A, Cost GJ, Caputo E, Li J, et al. (1998) Designer deletion strains derived from Saccharomyces cerevisiae S288C: a useful set of strains and plasmids for PCR-mediated gene disruption and other applications. Yeast 14: 115 132.
32. Gietz D, St Jean A, Woods RA, Schiestl RH (1992) Improved method for high efficiency transformation of intact yeast cells. Nucleic Acids Res 20: 1425.
33. MacKay VL, Welch SK, Insley MY, Manney TR, Holly J, et al. (1988) The Saccharomyces cerevisiae BAR1 gene encodes an exported protein with homology to pepsin. Proc Natl Acad Sci USA 85: 55 59.
34. Winzeler EA, Shoemaker DD, Astromoff A, Liang H, Anderson K, et al. (1999) Functional characterization of the S. cerevisiae genome by gene deletion and parallel analysis. Science 285: 901 906.
35. Ishii J, Matsumura S, Kimura S, Tatematsu K, Kuroda S, et al. (2006) Quantitative and dynamic analyses of G protein-coupled receptor signaling in yeast using Fus1, enhanced green fluorescence protein (EGFP), and His3 fusion protein. Biotechnol Prog 22: 954 960.
36. Ishii J, Izawa K, Matsumura S, Wakamura K, Tanino T, et al. (2009) A simple and immediate method for simultaneously evaluating expression level and plasmid maintenance in yeast. J Biochem 145: 701 708.

Analytical Biochemistry 426 (2012) 129–133

Contents lists available at SciVerse ScienceDirect

Analytical Biochemistry

journal homepage: www.elsevier.com/locate/yabio

Improved identification of agonist-mediated $G\alpha_i$-specific human G-protein-coupled receptor signaling in yeast cells by flow cytometry

Jun Ishii [a], Miyuki Moriguchi [b], Kiyotaka Y. Hara [a], Seiji Shibasaki [c], Hideki Fukuda [b], Akihiko Kondo [b,*]

[a] Organization of Advanced Science and Technology, Kobe University, Nada, Kobe 657-8501, Japan
[b] Department of Chemical Science and Engineering, Graduate School of Engineering, Kobe University, Nada, Kobe 657-8501, Japan
[c] Department of Pharmacy, School of Pharmacy, Hyogo University of Health Sciences, Chuo, Kobe 650-8530, Japan

ARTICLE INFO

Article history:
Received 13 February 2012
Received in revised form 3 April 2012
Accepted 5 April 2012
Available online 11 April 2012

Keywords:
G-protein-coupled receptor
Yeast
Signaling assay
Flow cytometry

ABSTRACT

Flow cytometry enables comparative quantification, population analysis, and high-throughput screening of agonist-mediated G-protein-coupled receptor (GPCR) signaling in genetically engineered yeasts. By using flow cytometry, we found that transformation of yeast cells with a low plasmid number is critical both for the construction of large screening libraries and for stable signal transmission in cell ensembles. Based on these findings, we constructed an engineered yeast strain for the improved identification of signal promotion by $G\alpha_i$-specific human GPCRs using flow cytometry.

G-protein-coupled receptors (GPCRs)[1] regulate various physiological processes, including taste, smell, vision, heart rate, blood pressure, neurotransmission, and cell growth, by responding to external stimuli [1]. Therefore, GPCRs are widely studied as major molecular targets in drug discovery research [2]. GPCRs are cell surface 7-transmembrane receptors that transduce signals via heterotrimeric guanine nucleotide binding proteins (G-proteins) comprising Gα-, Gβ- and Gγ-subunits in all eukaryotes [3].

The eukaryotic unicellular yeast, *Saccharomyces cerevisiae*, is a typical host cell used to study GPCRs at the molecular level. Compared with mammalian cell lines, *S. cerevisiae* provides a simple and predictive way in which to study GPCR signaling because it expresses only one kind of G-protein [4–6]. In addition, *S. cerevisiae* offers a crucial advantage for the screening of functional residues [7,8] and ligand binding [9,10] due to its rapid proliferation and amenability to genetic manipulation compared with other eukaryotes.

In general, reporter genes such as *HIS3* (auxotrophy), *lacZ* (colorimetry), and *luc* (luminometry) are often used to detect the activation of signaling pathways by heterologously expressed GPCRs in yeast cells [7–11]. These reporter genes offer comprehensive screening, comparative quantification, and extremely high detection sensitivity, respectively. In contrast, we have developed a signal-responsive assay system using the green fluorescent protein (*GFP*) gene as the reporter (Fig. 1) [4–6,12–15]. This system is applicable to flow cytometry and, therefore, enables comparative quantification, population analysis, and quantitative high-throughput screening to be performed [16–19]. To date, we have engineered several yeast strains to express heterologous GPCRs that activate signaling pathways in response to agonist stimulation [4–6,12–15]. However, we have not compared the relative suitability of these strains for flow cytometry.

In the current study, therefore, we evaluated a selection of these engineered yeast strains by flow cytometry. The index parameters, active cell population (proportion of signal-activated cells to total cells) and average GFP intensity (or signal-to-noise (S/N) ratio), were analyzed by flow cytometry in 10,000 cells treated with agonists. Because transformation efficiency is an important factor for library construction, colony-forming unit efficiency was also determined by counting the number of colonies generated following transformation of yeast cells with plasmids encoding heterologous GPCRs.

Materials and methods

Media

Synthetic dextrose (SD) medium contained 6.7 g/L yeast nitrogen base without amino acids (YNB, BD Diagnostic Systems,

* Corresponding author. Fax: +81 78 803 6196.
E-mail address: akondo@kobe-u.ac.jp (A. Kondo).

[1] *Abbreviations used:* GPCR, G-protein-coupled receptor; G-protein, guanine nucleotide binding protein; GFP, green fluorescent protein; SD, synthetic dextrose; SC, synthetic complete; AP, alkaline phosphatase; SSTR5, somatostatin receptor subtype 5; 5-FOA, 5-fluoroorotic acid; S-14, somatostatin 14; Gi3tp, Gpa1/$G\alpha_{i3}$ transplant; S/N, signal-to-noise.

0003-2697/$ - see front matter © 2012 Elsevier Inc. All rights reserved.
http://dx.doi.org/10.1016/j.ab.2012.04.012

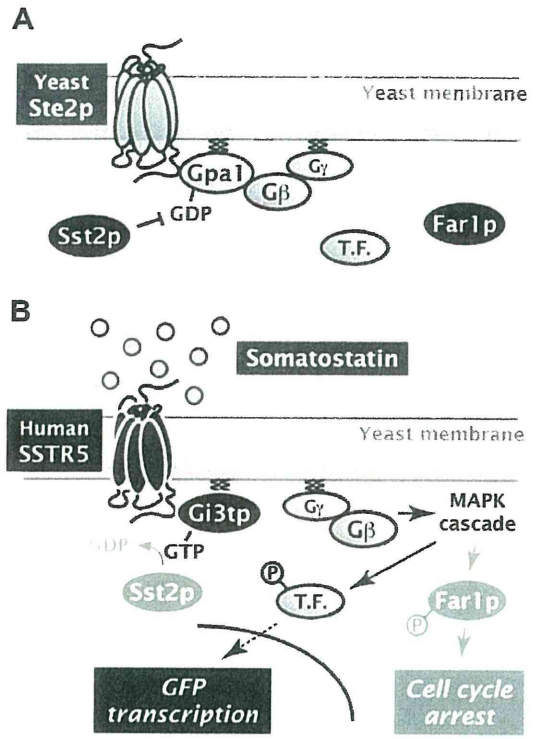

Fig.1. Outline of engineering strategy for SSTR5 signaling assay. (A) Schematic representation of major proteins involved in pheromone signal transduction in wild-type yeast. Yeast Ste2p, yeast endogenous GPCR; Gpa1, yeast endogenous Gα-subunit; Sst2p, Gpa1-specific GTPase-activating protein (a member of regulator of G-protein signaling (RGS) family that stimulates hydrolysis of GTP to GDP); Far1p, cyclin-dependent kinase inhibitor (mediates cell cycle arrest in response to pheromone signaling); T.F., transcription factor. (B) Schematic representation of engineered components of SSTR5 signaling assays. Yeast Ste2p was deleted to avoid competitive expression by the endogenous yeast GPCR. Alternatively, human SSTR5 was expressed from a multicopy episomal plasmid under the control of the constitutive *PGK1* promoter. A yeast–human chimeric G-protein in which the carboxyl-terminal 5 amino acid residues of Gpa1p were replaced by the equivalent residues to the human $G\alpha_{i3}$ (Gpa1/$G\alpha_{i3}$ transplant, Gi3tp) was substituted for Gpa1p. Sst2p was deleted to confer hypersensitivity to agonists. Far1p was deleted not only to promote cell cycle progression by avoiding G1 arrest even in signal-activated states but also to allow the recovery of episomal plasmids from signal-activated yeast cells, which is important for extensive screening. *GFP* reporter gene under the control of signal-responsive *FIG1* promoter was used to sense the SSTR5 signaling in the presence of somatostatin.

Sparks, MD, USA) and 20 g/L glucose. For SDM71 medium, 200 mM 3-(*N*-morpholino)-2-hydroxypropanesulfonic acid (Mopso, Nacalai Tesque, Kyoto, Japan) was added to SD medium to adjust the pH to 7.1. Amino acids and nucleotides (20 mg/L histidine, 60 mg/L leucine, 20 mg/L methionine, and 20 mg/L uracil) were supplemented into each medium to provide the relevant auxotrophic components. For synthetic complete (SC) medium, a variety of nutrients, including adenine, uracil, inositol, and *p*-aminobenzoic acid, as well as a complete range of amino acids were added into SD medium. To produce solid medium, 2% (w/v) agar was added when appropriate.

Plasmid constructions

All plasmids used in this study are listed in Table 1. All primers used for plasmid construction are listed in Supplementary Table 1 (see Supplementary material). A flow diagram for plasmid construction by the replacement of Gpa1p with Gi3tp is presented in Supplementary Fig. 1. DNA fragments corresponding to the respective upstream and downstream regions of the *GPA1* gene (*GPA5′* and *GPA3′*, 500 bp each) were amplified from BY4741 [20] genomic DNA and digested with *SacI–XhoI* and *XhoI–SphI*, respectively. The digested fragments were then simultaneously inserted into the *SacI–SphI* sites of pUC19 (Takara Bio, Shiga, Japan) by connecting the *XhoI* sites to generate the pI-GPA5.3 plasmid. A DNA fragment corresponding to the *URA3* selectable marker (containing 50 nt of the homologous region directly upstream of *GPA3′*, *hr50*) was amplified from pRS406 (American Type Culture Collection, Manassas, VA, USA) and digested with *XhoI* and *SalI*. The digested fragment was then inserted into the *XhoI* site of alkaline phosphatase (AP)-treated pI-GPA5.3 to retain the *XhoI* site at the *GPA5′* side, yielding the pUI-GPA5.3 plasmid. A DNA fragment encoding the *Gi3tp* gene (Gpa1/$G\alpha_{i3}$ transplant; the coding sequence for the carboxyl-terminal 5 amino acid residues of Gpa1p (KIGII) was replaced by the equivalent human $G\alpha_{i3}$ residues (ECGLY) [21]) was amplified from pSL-Gi3tp [4] and digested with *XhoI*. The digested fragment was then inserted into the *XhoI* site of AP-treated pUI-GPA5.3 to connect to the start codon of the *Gi3tp* gene at the *GPA5′* side, creating the pUI2-Gi3tp plasmid. A DNA fragment encoding the human somatostatin receptor subtype 5 (*SSTR5*) gene was amplified from pBlue-SSTR5-HA [5] and digested with *NheI–BglII*. The digested fragment was then inserted into the same sites of pGK421 [4,5], yielding the pGK421-SSTR5 plasmid.

Yeast strains

All yeast strains used in this study were generated from the BY4741 parental strain [20] and are listed in Table 1. A flow diagram for the construction of the yeast strain by substituting Gi3tp for Gpa1p is presented in Supplementary Fig. 2 (see Supplementary material). Transformation with linear DNA fragments was performed using the lithium acetate method [22]. The DNA fragment containing *GPA5′-Gi3tp-hr50-URA3-GPA3′* was prepared by digestion of pUI2-Gi3tp at the *SpeI* and *AseI* sites located in the *GPA5′* and *GPA3′* regions, respectively. The prepared linear DNA fragment was used to transform the IMFD-70 strain [5], and the transformant was selected on solid SD medium lacking uracil. After confirming integration of the DNA in the correct orientation, the cells were maintained on SC medium containing 1 mg/ml 5-fluoroorotic acid (5-FOA, Fluorochem, Derbyshire, UK) to eliminate the *URA3* selectable marker between the *hr50* and *GPA3′* genes by homologous recombination with counter selection. The strain substituted with the *Gi3tp* gene for the *GPA1* gene was designated as IMFD-72. Transformation with plasmids was also performed using the lithium acetate method to obtain all transformants used for assays.

SSTR5 signaling assay

To assay signal transduction mediated by the human SSTR5 receptor, the transformants were grown in SD medium at 30 °C. Cells were then inoculated into 50 ml of SDM71 medium to give an initial optical density of 0.03 at 600 nm (OD_{600} = 0.03). Cultures were grown at 30 °C with shaking at 150 rpm overnight and harvested. After washing, the cells were adjusted to an OD_{600} = 10 with sterile water. The cell suspensions (10 μl, to give a final OD_{600} = 1) and 100 or 0 μM somatostatin 14 (S-14, Calbiochem/Merck4Biosciences, Darmstadt, Germany) (10 μl, to give a final concentration of 10 or 0 μM) were added into the wells of 96-well cluster dishes containing the fresh SDM71 medium (80 μl), and then the plates were incubated at 30 °C with shaking at 150 rpm for 4 h. The total cell suspension volumes (100 μl) were directly diluted into test tubes containing sheath solution, and GFP fluorescence was measured using a BD FACSCalibur flow cytometer (BD Biosciences, San Jose, CA, USA). The green fluorescence signal of 10,000 cells was excited with a 488-nm argon laser and collected

Table 1
Yeast strains and plasmids used in this study.

Strain or plasmid	Specific features
Yeast strains	
BY4741	*MATa his3Δ1 leu2Δ0 met15Δ0 ura3Δ0*
MI-150	BY4741 *gpa1Δ::kanMX4 sst2Δ ste2Δ*
IM-50	BY4741 *sst2Δ::AUR1-C ste2Δ::LEU2*
IMF-50	BY4741 *sst2Δ::AUR1-C ste2Δ::LEU2 fig1Δ::EGFP*
IMFD-50	BY4741 *sst2Δ::AUR1-C ste2Δ::LEU2 fig1Δ::EGFP his3Δ::P_{FIG1}-EGFP*
IMFD-70	BY4741 *sst2Δ::AUR1-C ste2Δ::LEU2 fig1Δ::EGFP his3Δ::P_{FIG1}-EGFP far1Δ*
IMFD-72	BY4741 *sst2Δ::AUR1-C ste2Δ::LEU2 fig1Δ::EGFP his3Δ::P_{FIG1}-EGFP far1Δ gpa1Δ::Gi3tp*
Plasmids	
pUC19	Cloning vector
pI-GPA5.3	*GPA5′-GPA3′* in pUC19
pUI-GPA5.3	*GPA5′-hr50-URA3-GPA3′* in pUC19
pUI2-Gi3tp	*GPA5′-Gi3tp-hr50-URA3-GPA3′* in pUC19
pGK421	Expression vector containing *PGK1* promoter, 2μ origin and *MET15* marker
pGK421-SSTR5	Human SSTR5 receptor expression, *PGK1* promoter, 2μ origin and *MET15* marker
pSL-Gi3tp	Yeast–human chimeric Gα (Gi3tp) expression, *GPA1* promoter, *CEN/ARS* origin and *LEU2* marker
pSL-GPA1	Yeast endogenous Gα (Gpa1p) expression, *GPA1* promoter, *CEN/ARS* origin and *LEU2* marker
pMHG-FIG1	*GFP* reporter gene expression, *FIG1* promoter, 2μ origin and *HIS3* marker

through a 530/30-nm bandpass (FL1) filter. The data were analyzed using FlowJo software (version 8.5.3, Tree Star, Ashland, OR, USA).

Measurement of colony-forming unit efficiency

Cells were transformed with 1 μl of each plasmid (1 μg/μl) and selected on appropriate SD selectable solid medium at 30 °C for 2 to 4 days. Transformation of plasmids was performed using the lithium acetate method. Colony-forming units were determined from the numbers of colonies generated on the SD selectable solid medium.

Results and discussion

To compare the strains by flow cytometry, human SSTR5, which endogenously signals via $G\alpha_i$ [23], was selected as a model for heterologous GPCRs expressed in engineered yeast cells. The natural peptide ligand, S-14 [24], was used as the agonist. In all engineered yeast strains, the *ste2Δ* allele was conferred to avoid the competitive expression of the endogenous yeast GPCR (Ste2p) (Fig. 1). The human SSTR5 receptor was expressed via a multicopy episomal plasmid under the control of constitutive *PGK1* promoter (pGK421-SSTR5) (Table 1).

Whereas the human SSTR5 receptor is known to transduce signals in yeast cells through the endogenous yeast Gα-subunit (Gpa1p) [4–6,21], the yeast–human chimeric G-protein, in which the carboxyl-terminal 5 amino acid residues of Gpa1p are replaced by the equivalent residues from human $G\alpha_{i3}$ ($Gpa1/G\alpha_{i3}$ transplant, Gi3tp) (Fig. 1), has been shown to improve signal transmission via $G\alpha_i$-specific SSTR5 in yeast [21]. We previously constructed single-copy episomal plasmids that expressed the yeast–human chimeric Gi3tp or the yeast wild-type Gpa1p under the control of *GPA1* promoter (pSL-Gi3tp and pSL-GPA1) and a yeast strain (MI-150) with *gpa1Δ sst2Δ ste2Δ* triple deletion alleles [4] (Table 1). The *gpa1Δ* allele excluded signal transmission through the intrinsic yeast Gα-subunit, and the *sst2Δ* allele conferred hypersensitivity toward agonists by diminishing the activity of Gpa1-specific GTPase-activating protein [3,4] (Fig. 1). In addition, we also previously constructed a multicopy episomal plasmid (pMHG-FIG1) to express the *GFP* reporter gene under the control of the signal-responsive *FIG1* promoter [4] (Table 1).

First, we confirmed signal transduction by the MI-150 yeast strains transformed with pGK421-SSTR5, pSL-Gi3tp (or pSL-GPA1), and pMHG-FIG1 using a BD FACSCalibur flow cytometer and FlowJo software. We observed that S-14 mediated signal transduction via Gi3tp in the triple transformants by an increase in the active cell population compared with control cells (36.42–48.99%) (Fig. 2A and B). Next, we introduced pGK421-SSTR5 and pMHG-FIG1 into the yeast strain harboring *sst2Δ ste2Δ* double deletion alleles (IM-50) that expressed endogenous Gpa1p [14] (Table 1). Compared with the MI-150 triple transformant, this double transformant improved the active cell population (36.42–74.69%) that responded to S-14 (Fig. 2A and C). This observation was also supported by the increased average GFP intensity (signal-to-noise (S/N) ratio) in 10,000 cells (Fig. 3A and C). These

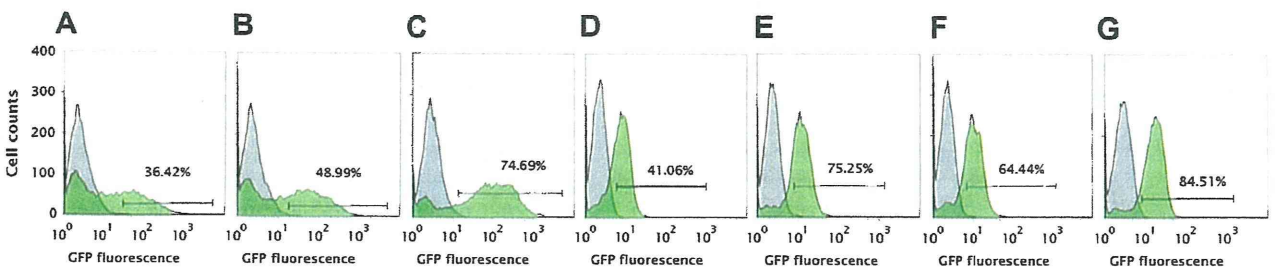

Fig.2. Active cell populations. Signal transduction in SSTR-expressing yeast cells was invoked with 10 μM S-14 and analyzed by a flow cytometer as described in Materials and Methods: (A) MI-150/pGK421-SSTR5/pSL-GPA1/pMHG-FIG1; (B) MI-150/pGK421-SSTR5/pSL-Gi3tp/pMHG-FIG1; (C) IM-50/pGK421-SSTR5/pMHG-FIG1; (D) IMF-50/pGK421-SSTR5; (E) IMFD-50/pGK421-SSTR5; (F) IMFD-70/pGK421-SSTR5; (G) IMFD-72/pGK421-SSTR5. Filled green and gray histograms represent the yeast cells incubated in pH-adjusted medium with and without S-14, respectively. Active cell populations were defined as the cell populations included in the areas where the populations of signal-unpromoted cells in the absence of S-14 were less than 0.1%. (For interpretation of the references to color in this figure legend, the reader is referred to the Web version of this article.)

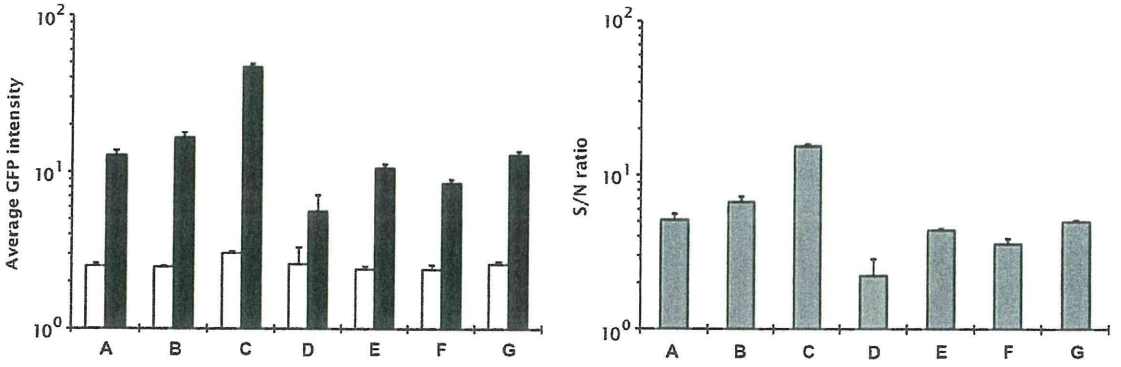

Fig.3. Average GFP intensities (left) and S/N ratios (right). Signal transduction in SSTR5-expressing yeast cells was invoked with 10 μM S-14 and analyzed by a flow cytometer as described in Materials and Methods: (A) MI-150/pGK421-SSTR5/pSL-GPA1/pMHG-FIG1; (B) MI-150/pGK421-SSTR5/pSL-Gi3tp/pMHG-FIG1; (C) IM-50/pGK421-SSTR5/pMHG-FIG1; (D) IMF-50/pGK421-SSTR5; (E) IMFD-50/pGK421-SSTR5; (F) IMFD-70/pGK421-SSTR5; (G) IMFD-72/pGK421-SSTR5. Black and white bars present the average GFP intensities of the yeast cells incubated in pH-adjusted medium with and without S-14, respectively. Gray bars present the S/N ratios. Error bars represent the standard deviations ($n = 3$).

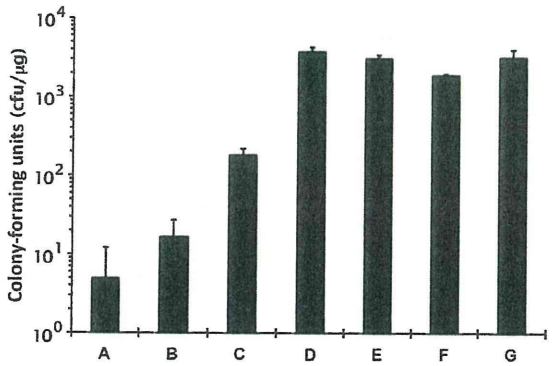

Fig.4. Colony-forming units obtained by transformation of yeast cells. Cells were transformed with 1 μl of each plasmid (1 μg/μl) as described in Materials and Methods: (A) MI-150/pGK421-SSTR5/pSL-GPA1/pMHG-FIG1; (B) MI-150/pGK421-SSTR5/pSL-Gi3tp/pMHG-FIG1; (C) IM-50/pGK421-SSTR5/pMHG-FIG1; (D) IMF-50/pGK421-SSTR5; (E) IMFD-50/pGK421-SSTR5; (F) IMFD-70/pGK421-SSTR5; (G) IMFD-72/pGK421-SSTR5. Colony-forming units were determined as the numbers of observed colonies on the appropriate selectable medium. Error bars represent the standard deviations ($n = 3$).

results suggest that recombinant protein expression by several plasmids attenuates the phenotypic stability of the yeast strains. Moreover, the IM-50 double transformant showed a higher score in the colony-forming unit assay than the MI-150 triple transformant (Fig. 4A–C), indicating that the transformation of yeast cells with a lower plasmid number is more efficient. Therefore, transformation with less than three plasmids may be more suitable for construction of the large libraries required to screen candidate receptor mutants and ligand substitutes.

Because of the results of the colony-forming unit assays from yeast strains transformed with two or three plasmids, we subsequently tested the engineered yeast strains that mediate signal transduction via one introduced plasmid only. The IMF-50 and IMFD-50 strains possess identical deletion alleles, including *sst2Δ* and *ste2Δ* as well as the *fig1Δ* deletion generated by replacing the genomic *FIG1* gene with the *GFP* reporter gene to enable agonist-mediated signal transduction to be detected by the appearance of green fluorescence [5] (Table 1). However, the IMFD-50 strain has an apparent difference with the IMF-50 strain conferred by an additional cassette that expresses the *GFP* reporter gene under the control of the signal-responsive *FIG1* promoter inserted into the function-deficient *HIS3* (*his3Δ1*) genomic locus [5] (Table 1). Compared with the strains harboring two or three plasmids, the IMF-50 strain harboring pGK421-SSTR5 exhibited a lower active cell population (41.06%) and a lower average GFP intensity (S/N ratio) following stimulation by S-14 (Figs. 2D and 3D). However, the colony-forming unit score of the IMF-50 strain was substantially augmented (Fig. 4D). In the presence of S-14, the IMFD-50 strain harboring pGK421-SSTR5 displayed higher values for active cell population (75.25%) and average GFP intensity (S/N ratio) than the IMF-50 strain harboring pGK421-SSTR5 as well as an elevated colony-forming unit score (Figs. 2E, 3E, and 4E). These results indicate that the two *FIG1* promoter-driven *GFP* reporter gene cassettes integrated into the chromosomes of the IMFD-50 strain enhance the green fluorescence signal in response to GPCR-mediated signal transduction.

Next, we evaluated the IMFD-70 strain (derived from the IMFD-50), which harbors a deletion in the *FAR1* gene that encodes a cyclin-dependent kinase inhibitor and mediates cell cycle arrest in response to receptor activation [3,5] (Table 1). Whereas the *far1Δ* allele promotes cell cycle progression by avoiding G1 arrest even in signal-activated states (Fig. 1), it also allows the recovery of episomal plasmids from signal-activated yeast cells that is important for extensive screening [14]. The IMFD-70 strain harboring pGK421-SSTR5 exhibited similar characteristics to the *FAR1*-intact IMFD-50 strain harboring pGK421-SSTR5 (Figs. 2F, 3F, and 4F), although the active cell population that responded to S-14 was slightly decreased by the *FAR1* deletion (64.44%) (Fig. 2F). Therefore, we attempted to elevate the active cell population while maintaining the colony-forming unit efficiency.

We constructed a new strain that expressed the yeast–human chimeric Gi3tp in place of yeast endogenous Gpa1p under the control of the genomic *GPA1* locus. Using the IMFD-70 strain, the gene encoding Gi3tp was substituted for the chromosomal *GPA1* gene by homologous recombination via the marker recycling method [25] to create the IMFD-72 yeast strain (Table 1 and Fig. 1). As expected from the results with episomal plasmids (Fig. 2A and B), the IMFD-72 strain harboring pGK421-SSTR5 substantially improved the active cell population while maintaining the colony-forming unit efficiency (Figs. 2G and 4G). It is notable that the active cell population value was the highest (84.51%) among all tested strains (Fig. 2A–G). These results indicate that the chromosomally integrated yeast–human chimeric *Gi3tp* gene contributed to the coupling of the $G\alpha_i$-specific human SSTR5 receptor. In addition, the lower number of plasmids in the IMFD-72 transformant also enabled stable signal transduction in the cell population and improved the colony-forming unit efficiency. Because the stable signal transduction (active cell population) and the colony-forming unit are more critical for the screening with flow cytometric

separation rather than the average GFP intensity (S/N ratio), the IMFD-72 yeast strain would be able to identify the $G\alpha_i$-specific receptor mutants and the ligand substitutes.

Conclusion

We used flow cytometry to evaluate the ability of previously constructed yeast strains to sense agonist-mediated signal transduction by genetically expressed human SSTR5. As a result, we found that reducing the number of plasmids introduced into the engineered yeast cells was a critical factor not only for the construction of the large library required for screening but also for enabling stable transmission of the signal in the cell ensembles. Based on these findings, we constructed the engineered IMFD-72 yeast strain by chromosomal integration of the yeast–human chimeric *Gi3tp* gene as a substitute for the *GPA1* gene and two cassettes of the signal-responsive *GFP* reporter gene in addition to the *far1Δ gpa1Δ sst2Δ* and *ste2Δ* deletion alleles. This IMFD-72 strain enabled improved flow cytometric separation to identify signal transduction mediated by the $G\alpha_i$-specific human SSTR5 GPCR. Because the impact of the yeast–human chimeric Gi3tp G-protein has been demonstrated for a variety of $G\alpha_i$-specific human GPCRs [21], the IMFD-72 strain should be applicable for the screening of human $G\alpha_i$-specific receptors other than SSTR5.

Acknowledgments

This work was supported mainly by a Grant-in-Aid for Scientific Research on Priority Areas (Life Surveyor) from the Ministry of Education, Culture, Sports, Science, and Technology (MEXT). It was also funded in part by the Special Coordination Funds for Promoting Science and Technology, Creation of Innovation Centers for Advanced Interdisciplinary Research Areas (Innovative Bioproduction Kobe, iBioK) from the MEXT of Japan, and AS ONE Corporation.

Appendix A. Supplementary data

Supplementary data associated with this article can be found, in the online version, at http://dx.doi.org/10.1016/j.ab.2012.04.012.

References

[1] O. Vögler, J.M. Barceló, C. Ribas, P.V. Escribá, Membrane interactions of G proteins and other related proteins, Biochim. Biophys. Acta 1778 (2008) 1640–1652.
[2] R. Heilker, M. Wolff, C.S. Tautermann, M. Bieler, G-protein-coupled receptor-focused drug discovery using a target class platform approach, Drug Discov. Today 14 (2009) 231–240.
[3] J. Ishii, N. Fukuda, T. Tanaka, C. Ogino, A. Kondo, Protein–protein interactions and selection: yeast-based approaches that exploit guanine nucleotide-binding protein signaling, FEBS J. 277 (2010) 1982–1995.
[4] Y. Iguchi, J. Ishii, H. Nakayama, A. Ishikura, K. Izawa, T. Tanaka, C. Ogino, A. Kondo, Control of signalling properties of human somatostatin receptor subtype-5 by additional signal sequences on its amino-terminus in yeast, J. Biochem. 147 (2010) 875–884.
[5] S. Togawa, J. Ishii, A. Ishikura, T. Tanaka, C. Ogino, A. Kondo, Importance of asparagine residues at positions 13 and 26 on the amino-terminal domain of human somatostatin receptor subtype-5 in signaling, J. Biochem. 147 (2010) 867–873.
[6] N. Fukuda, J. Ishii, M. Kaishima, A. Kondo, Amplification of agonist stimulation of human G-protein-coupled receptor signaling in yeast, Anal. Biochem. 417 (2011) 182–187.
[7] B. Li, M. Scarselli, C.D. Knudsen, S.K. Kim, K.A. Jacobson, S.M. McMillin, J. Wess, Rapid identification of functionally critical amino acids in a G protein-coupled receptor, Nat. Methods 4 (2007) 169–174.
[8] T.J. Baranski, P. Herzmark, O. Lichtarge, B.O. Gerber, J. Trueheart, E.C. Meng, T. Iiri, S.P. Sheikh, H.R. Bourne, C5a receptor activation: genetic identification of critical residues in four transmembrane helices, J. Biol. Chem. 274 (1999) 15757–15765.
[9] C. Klein, J.I. Paul, K. Sauvé, M.M. Schmidt, L. Arcangeli, J. Ransom, J. Trueheart, J.P. Manfredi, J.R. Broach, A.J. Murphy, Identification of surrogate agonists for the human FPRL-1 receptor by autocrine selection in yeast, Nat. Biotechnol. 16 (1998) 1334–1337.
[10] J.P. Manfredi, C. Klein, J.J. Herrero, D.R. Byrd, J. Trueheart, W.T. Wiesler, D.M. Fowlkes, J.R. Broach, Yeast α mating factor structure–activity relationship derived from genetically selected peptide agonists and antagonists of Ste2p, Mol. Cell. Biol. 16 (1996) 4700–4709.
[11] Y. Fukutani, T. Nakamura, M. Yorozu, J. Ishii, A. Kondo, M. Yohda, The N-terminal replacement of an olfactory receptor for the development of a yeast-based biomimetic odor sensor, Biotechnol. Bioeng. 109 (2012) 205–212.
[12] J. Ishii, N. Yoshimoto, K. Tatematsu, S. Kuroda, C. Ogino, H. Fukuda, A. Kondo, Cell wall trapping of autocrine peptides for human G-protein-coupled receptors on the yeast cell surface, in press.
[13] S. Ryo, J. Ishii, Y. Iguchi, N. Fukuda, A. Kondo, Transplantation of the GAL regulon into G-protein signaling circuitry in yeast, Anal. Biochem. 424 (2012) 27–31.
[14] J. Ishii, T. Tanaka, S. Matsumura, K. Tatematsu, S. Kuroda, C. Ogino, H. Fukuda, A. Kondo, Yeast-based fluorescence reporter assay of G protein-coupled receptor signalling for flow cytometric screening: *FAR1*-disruption recovers loss of episomal plasmid caused by signalling in yeast, J. Biochem. 143 (2008) 667–674.
[15] J. Ishii, S. Matsumura, S. Kimura, K. Tatematsu, S. Kuroda, H. Fukuda, A. Kondo, Quantitative and dynamic analyses of G protein-coupled receptor signaling in yeast using Fus1, enhanced green fluorescence protein (EGFP), and His3 fusion protein, Biotechnol. Prog. 22 (2006) 954–960.
[16] S. Müller, G. Nebe-von-Caron, Functional single-cell analyses: flow cytometry and cell sorting of microbial populations and communities, FEMS Microbiol. Rev. 34 (2010) 554–587.
[17] J. Ishii, K. Izawa, S. Matsumura, K. Wakamura, T. Tanino, T. Tanaka, C. Ogino, H. Fukuda, A. Kondo, A simple and immediate method for simultaneously evaluating expression level and plasmid maintenance in yeast, J. Biochem. 145 (2009) 701–708.
[18] N. Fukuda, J. Ishii, S. Shibasaki, M. Ueda, H. Fukuda, A. Kondo, High-efficiency recovery of target cells using improved yeast display system for detection of protein–protein interactions, Appl. Microbiol. Biotechnol. 76 (2007) 151–158.
[19] S. Shibasaki, A. Kawabata, J. Ishii, S. Yagi, T. Kadonosono, M. Kato, N. Fukuda, A. Kondo, M. Ueda, Construction of a novel synergistic system for production and recovery of secreted recombinant proteins by the cell surface engineering, Appl. Microbiol. Biotechnol. 75 (2007) 821–828.
[20] C.B. Brachmann, A. Davies, G.J. Cost, E. Caputo, J. Li, P. Hieter, J.D. Boeke, Designer deletion strains derived from *Saccharomyces cerevisiae* S288C: a useful set of strains and plasmids for PCR-mediated gene disruption and other applications, Yeast 14 (1998) 115–132.
[21] A.J. Brown, S.L. Dyos, M.S. Whiteway, J.H. White, M.A. Watson, M. Marzioch, J.J. Clare, D.J. Cousens, C. Paddon, C. Plumpton, M.A. Romanos, S.J. Dowell, Functional coupling of mammalian receptors to the yeast mating pathway using novel yeast/mammalian G protein α-subunit chimeras, Yeast 16 (2000) 11–22.
[22] D. Gietz, A. St Jean, R.A. Woods, R.H. Schiestl, Improved method for high efficiency transformation of intact yeast cells, Nucleic Acids Res. 20 (1992) 1425.
[23] L.N. Møller, C.E. Stidsen, B. Hartmann, J.J. Holst, Somatostatin receptors, Biochim. Biophys. Acta 1616 (2003) 1–84.
[24] R. Burgus, N. Ling, M. Butcher, R. Guillemin, Primary structure of somatostatin, a hypothalamic peptide that inhibits the secretion of pituitary growth hormone, Proc. Natl. Acad. Sci. USA 70 (1973) 684–688.
[25] R. Akada, T. Kitagawa, S. Kaneko, D. Toyonaga, S. Ito, Y. Kakihara, H. Hoshida, S. Morimura, A. Kondo, K. Kida, PCR-mediated seamless gene deletion and marker recycling in *Saccharomyces cerevisiae*, Yeast 23 (2006) 399–405.

Analytical Biochemistry 424 (2012) 27–31

Contents lists available at SciVerse ScienceDirect

Analytical Biochemistry

journal homepage: www.elsevier.com/locate/yabio

Transplantation of the GAL regulon into G-protein signaling circuitry in yeast

Shintaro Ryo [a], Jun Ishii [b], Yusuke Iguchi [a], Nobuo Fukuda [a], Akihiko Kondo [a,*]

[a] Department of Chemical Science and Engineering, Graduate School of Engineering, Kobe University, Nada, Kobe 657-8501, Japan
[b] Organization of Advanced Science and Technology, Kobe University, Nada, Kobe 657-8501, Japan

ARTICLE INFO

Article history:
Received 10 December 2011
Accepted 3 February 2012
Available online 13 February 2012

Keywords:
Yeast
G-protein-coupled receptor (GPCR)
Pheromone signaling
GAL regulon
Flow cytometry

ABSTRACT

Here we present a successful transplantation of the GAL genetic regulatory circuitry into the G-protein signaling pathway in yeast. The GAL regulon represents a strictly regulated transcriptional mechanism that we have transplanted into yeast to create a highly robust induction system to assist the detection of on–off switching in G-protein signaling. In our system, we engineered yeast to drive the positive GAL regulatory gene in response to agonist-promoted G-protein signaling and to induce transcription of a green fluorescent protein (*GFP*) reporter gene under the control of the GAL structural gene promoter. Consequently, in response to agonist stimulation of G-protein-coupled receptors (GPCRs), the engineered yeast achieved more than a 150-fold increase in reporter intensity in up to 98% of cells, as determined by flow cytometric sorting. Surprisingly, agonist-stimulated induction of the *GFP* reporter gene was higher than that by galactose. Our approach to boost reporter gene induction could be applicable in establishing more efficient yeast-based flow cytometric screening systems for agonistic ligands for heterogeneous GPCRs.

Transcriptional regulation in eukaryotes often requires the cooperation of many proteins to bind to the upstream region of a gene [1]. Such highly regulated transcriptional networks frequently possess negative feedback or positive feedback loops capable of suppressing transcriptional noise or amplifying transcription [1,2].

The GAL regulatory network in *Saccharomyces cerevisiae* is one of the most studied genetic networks [3]. The structural genes (*GAL2*, *GAL1*, *GAL7*, and *GAL10*) of the GAL network operate to regulate galactose transport and metabolism [1,2], with their expression regulated by the presence of glucose and galactose [4]. The regulatory genes (*GAL4*, *GAL80*, and *GAL3*) involve a mechanism for swift transcriptional activation of the GAL genes in the presence of galactose [5]. The transcriptional activator Gal4 binds to the upstream activation sequence (UAS_{GAL})[1] and transcribes the GAL genes, whereas Gal80 and Gal3 provide negative and positive feedback on GAL expression, respectively [2,3]. In the absence of galactose, Gal80 interacts with Gal4 to inhibit its activity, whereas the galactose-bound Gal3 interacts with Gal80 to relieve the inhibition of Gal4 and permit the expression of the GAL genes [5] (Fig. 1A). Because the GAL genetic circuitry is well characterized and strictly regulated, the promoters of GAL genes such as *GAL1*, which induces intensive transcriptional activation, are often used as a highly robust induction system. Yeast contains guanine nucleotide-binding proteins (G-proteins) and G-protein-coupled receptors (GPCRs) as peripheral membrane and trans-membrane proteins. In humans, GPCRs are involved in the control of many physiological functions such as taste, smell, vision, heart rate, blood pressure, neurotransmission, and cell growth [6]; therefore, they are considered as attractive pharmaceutical and therapeutic targets [7]. The eukaryotic unicellular *S. cerevisiae* is a familiar host cell system to study GPCR signaling because its uncompetitive and monopolistic G-protein signaling pathway (pheromone signaling pathway) can simplify the analyses of complicated mammalian GPCR signaling systems [8–12]. The existence of signal-responsive assay systems using transcriptional reporter genes such as *HIS3* (auxotrophy), *lacZ* (colorimetry), and *luc* (luminometry) means that yeast is an easy-to-use analytical tool [12–15]. In general, because high sensitivity is a requirement of most assays, reporter sensitivity is an important determinant when considering an experimental approach.

Here, we report the successful transplantation of the GAL genetic regulatory circuitry into the G-protein signaling pathway in yeast. We were able to engineer transcriptional activation of the GAL regulon downstream of GPCR activation (Fig. 1B–D) in order to produce a robust and inducible expression system capable of significant reporter expression even in the absence of galactose. In the current study, the endogenous yeast GPCR (Ste2) and its natural ligand (α-factor) were used to demonstrate our concept. In addition, we used a green fluorescent protein (*GFP*) reporter gene with the future aim of applying this system to quantitative, high-throughput screening using flow cytometry.

* Corresponding author. Fax: +81 78 803 6196.
E-mail address: akondo@kobe-u.ac.jp (A. Kondo).

[1] *Abbreviations used:* UAS, upstream activation sequence; G-protein, guanine nucleotide-binding protein; GPCR, G-protein-coupled receptor; YNB, yeast nitrogen base without amino acids; GFP, green fluorescent protein; EGFP, enhanced green fluorescent protein; PCR, polymerase chain reaction; $Gal3^c$, constitutively active Gal3 mutant; EC_{50}, half-maximal effective concentration.

0003-2697/$ - see front matter © 2012 Elsevier Inc. All rights reserved.
doi:10.1016/j.ab.2012.02.005

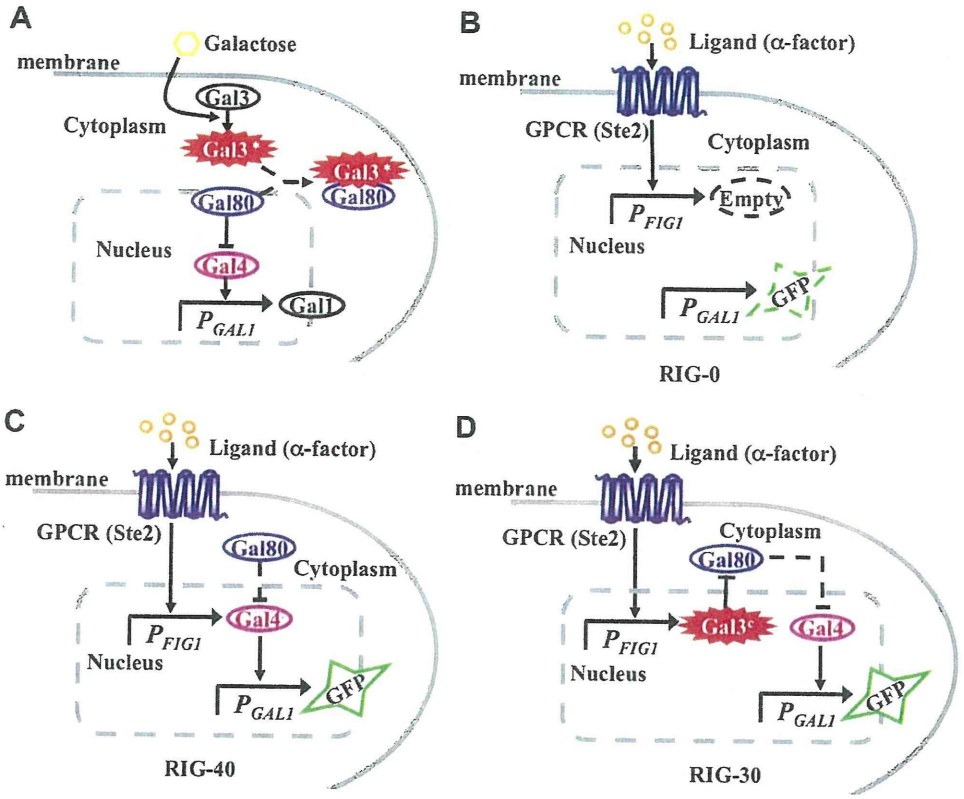

Fig.1. Outline of the experimental design. (A) GAL genetic regulatory network in wild-type yeast. The transcription of GAL structural genes (including *GAL1*) is strictly regulated by the GAL regulatory genes (*GAL4*, *GAL80*, and *GAL3*). Without galactose (in the presence of glucose), Gal80 binds to the transcriptional activator Gal4 and inhibits expression of *GAL1*. In the presence of galactose, the galactose-bound Gal3 (Gal3*) interacts with Gal80 and relieves the inhibition of Gal4, permitting the expression of *GAL1*. (B–D) Transplantation of GAL genetic regulatory circuitry into G-protein signaling pathway in yeast. (B) The RIG-0 control strain is engineered to express the *GFP* reporter gene under the control of the *GAL1* promoter. The RIG-0 control strain was used for construction of the RIG-40 and RIG-30 yeast strains. (C) The RIG-40 strain is engineered to express the transcriptional activator *GAL4* gene in response to an agonist-promoted signal from a GPCR. Signal-dependent Gal4 expression could induce *GFP* transcription due to a lack of inhibition of Gal80 (Gal4 repressor). (D) The RIG-30 strain is engineered to express a constitutively active mutant of Gal3 ($Gal3^c$) in response to an agonist-promoted signal from a GPCR. Signal-dependent expression of $Gal3^c$ then binds to Gal80, inhibiting its activity and inducing *GFP* transcription.

Materials and methods

Media

YPD medium contained 1% yeast extract (Nacalai Tesque, Kyoto, Japan), 2% peptone (BD Diagnostic Systems, Sparks, MD, USA), and 2% glucose. SD medium contained 0.67% yeast nitrogen base without amino acids (YNB) (BD Diagnostic Systems) and 2% glucose. SG medium contained 0.67% YNB and 2% galactose. SDLG medium contained 0.67% YNB, 3% glycerol, 0.05% glucose, and 2% lithium lactate (Sigma–Aldrich, St. Louis, MO, USA) [16]. Amino acids and nucleotides (20 mg/L histidine, 60 mg/L leucine, 20 mg/L methionine, and 20 mg/L uracil) were supplemented into each medium to lack the relevant auxotrophic components. For SDLG medium, amino acids complete drop-out mix was additionally supplemented to lack the relevant auxotrophic components.

Plasmid construction

All plasmids used in this study are summarized in Table 1. All primers used for the plasmid constructions are listed in Supplementary Table 1 in the supplementary material. The amplified DNA fragments encoding the *GAL1* promoter (600 bp) and the enhanced green fluorescent protein (*EGFP*) were digested with *Bam*HI and *Xba*I and with *Xba*I and *Sal*I, respectively, and were simultaneously inserted at *Bam*HI and *Sal*I sites into pUC19 vector (Takara Bio, Shiga, Japan), resulting in pUC19-12. The DNA fragments encoding the *URA3* selectable marker (with 50 nucleotides from the 5′ side of the *GAL1* terminator at the 5′ end) and the *GAL1* terminator (800 bp) were amplified by overlap polymerase chain reaction (PCR), and the conjugated fragment was inserted at *Sph*I and *Sal*I sites into pUC19-12, creating pGAL1pt–EGFP. The amplified DNA fragment encoding the *GAL3* gene was inserted at *Bam*HI and *Sac*II sites into pBlueScript II KS(+) vector (Agilent Technologies, Santa Clara, CA, USA), generating pBlue–GAL3. To introduce the S509P point mutation into the *GAL3* gene [16], QuikChange site-directed mutagenesis (Agilent Technologies) was carried out using pBlue–GAL3 as a template according to the manufacturer's protocol, creating pBlue–$GAL3^c$. The amplified DNA fragment corresponding to the *FIG1* promoter (600 bp) was inserted at *Eco*RI and *Sac*I sites into pUC19 vector, resulting in pUC19–FIG1p. The amplified DNA fragment containing the *URA3* selectable marker (with 40 nucleotides from the 5′ side of the *FIG1* terminator at the 5′ end) and the *FIG1* terminator (300 bp) from pFIG450GF [11] was inserted at *Sma*I and *Hin*dIII sites into pUC19–FIG1p, making pUC19–FIG1ptURA3. The amplified DNA fragment encoding the *GAL4* gene was inserted at *Sac*I and *Sma*I sites into pUC19–FIG1ptURA3, producing pFIG1pt–GAL4. The digested DNA fragment encoding the $GAL3^c$ gene was prepared from pBlue–$GAL3^c$ and inserted at *Sac*I and *Sma*I sites into pUC19–FIG1ptURA3, producing pFIG1pt–$GAL3^c$.

Yeast strain construction

Yeast strains used in this study are listed in Table 1. We used the lithium acetate method to transform these strains with linear

Table 1
Yeast strains and plasmids.

Strain or plasmid	Description	Reference
Strain		
BY4741	*MATa his*Δ*1 leu2*Δ*0 met15*Δ*0 ura3*Δ*0*	[19]
MI-7	BY4741 *sst2*Δ*::kanMX4 far1*Δ	This study
RIG-0	MI-7 *gal1*Δ*::EGFP*	This study
RIG-30	RIG-0 *fig1*Δ*::GAL3^c*	This study
RIG-40	RIG-0 *fig1*Δ*::GAL4*	This study
Plasmid		
pUC19	Cloning vector	Takara Bio
pUC19-12	P_{GAL1}*(600 bp)–EGFP* in pUC19	This study
pGAL1pt-EGFP	P_{GAL1}*(600 bp)–EGFP–*T_{GAL1}*(50 bp)-URA3–*T_{GAL1}*(800 bp)* in pUC19	This study
pBlueScript II KS(+)	Cloning vector	Agilent Technologies
pBlue-GAL3	*GAL3* in pBlueScript II KS(+)	This study
pBlue-GAL3^c	*GAL3^c* (S509P point mutation in Gal3) in pBlueScript II KS(+)	This study
pUC19-FIG1p	P_{FIG1}*(600 bp)* in pUC19	This study
pFIG450GF	P_{FIG1}*(450 bp)–EGFP–*T_{FIG1}*(40 bp)–URA3–*T_{FIG1}*(300 bp)* in pUC119	[11]
pUC19-FIG1ptURA3	P_{FIG1}*(600 bp)–*T_{FIG1}*(40 bp)–URA3–*T_{FIG1}*(300 bp)* in pUC19	This study
pFIG1pt-GAL4	P_{FIG1}*(600 bp)–GAL4–*T_{FIG1}*(40 bp)–URA3–*T_{FIG1}*(300 bp)* in pUC19	This study
pFIG1pt-GAL3^c	P_{FIG1}*(600 bp)–GAL3^c–*T_{FIG1}*(40 bp)–URA3–*T_{FIG1}*(300 bp)* in pUC19	This study

DNA fragments [17]. All homologous recombination procedures followed the marker recycle method [18] to eliminate and reuse the *URA3* selectable marker. To generate the MI-7 yeast strain, the *far1*Δ allele was inserted into an *sst2*Δ single mutant strain derived from BY4741 [19] (obtained from the *Saccharomyces* Genome Deletion Project [20]), essentially as described previously [10]. To construct the recombinant yeast strain in which the genomic *GAL1* gene was replaced by the *EGFP* reporter gene, the DNA fragment obtained by digesting pGAL1pt–EGFP with *Bgl*I and *Bgl*II was introduced into MI-7. We designated the *URA3*-eliminated strain as RIG-0. To produce the recombinant yeast strain in which the genomic *FIG1* gene was replaced by the *GAL4* gene, the DNA fragment obtained by digesting pFIG1pt–GAL4 with *Ahd*I and *Hin*dIII was introduced into RIG-0. We designated the *URA3*-eliminated strain as RIG-40. Similarly, to fabricate the recombinant yeast strain in which the genomic *FIG1* gene was replaced by the *GAL3^c* gene, the DNA fragment obtained by digesting pFIG1pt–GAL3^c with *Ahd*I and *Hin*dIII was introduced into RIG-0. We designated the *URA3*-eliminated strain as RIG-30.

Pheromone signaling assay

Recombinant yeast strains (RIG-0, RIG-30, and RIG-40) precultivated in YPD medium for 12 h were inoculated into 3 ml of SDLG medium containing indicated concentrations of α-factor (Zymo Research, Orange, CA, USA) to give an initial optical density of 0.1 at 600 nm. They were grown at 30 °C with shaking at 150 rpm for 18 h. Then, the cells were suspended into 1 ml of sheath solution, and GFP fluorescence was analyzed by a BD FACSCanto II flow cytometer equipped with a 488-nm blue laser (BD Biosciences, San Jose, CA, USA). The GFP fluorescence signal was collected through a 530/30-nm bandpass filter, and the mean of fluorescence intensity was defined as the GFP-A mean of 10,000 cells. The data were analyzed using BD FACSDiva software (version 5.0, BD Biosciences) and FlowJo software (version 8.5.3, Tree Star, Ashland, OR, USA).

Galactose-mediated induction of GAL regulon

RIG-0 yeast strain was grown in SD or SG medium without α-factor to check the induction level of the *GAL1* promoter by galactose. GFP fluorescence was measured as for the pheromone signaling assay.

Results and discussion

The aim of this study was to incorporate the GAL genetic regulatory circuitry into the G-protein signaling pathway in the yeast *S. cerevisiae* in order to establish a highly robust reporter gene assay system for detecting on–off switching in G-protein signaling, responding to agonist stimulation of GPCRs. To achieve this, we designed recombinant yeast strains to induce transcription of the genetically introduced GAL regulon in response to activation of the G-protein (pheromone) signaling pathway. As a specific strategy, yeast was engineered to express Gal4 or a constitutively active Gal3 mutant (Gal3^c) [16] under the control of the pheromone-responsive *FIG1* promoter, a commonly used reporter gene to detect G-protein signaling [10,11] (Fig. 1B–D). The overexpression of Gal4 was expected to directly activate the transcription of GAL genes (Fig. 1C), whereas the induction of Gal3^c was expected to promote transcription of GAL genes through the activation of Gal4 protein (Fig. 1D). We used the *GAL1* promoter, as the output of agonist stimulation, to induce expression of the *GFP* reporter gene (Fig. 1B–D).

First, we constructed the MI-7 yeast strain harboring *sst2*Δ and *far1*Δ double deletion alleles that confer advantages in GPCR signaling assays by increasing sensitivity to the agonistic ligand and inhibiting cell cycle arrest [21]. Using MI-7 as a backbone strain, we replaced the genomic *GAL1* gene with the *GFP* reporter gene, generating the RIG-0 yeast strain (Table 1). To check the induction

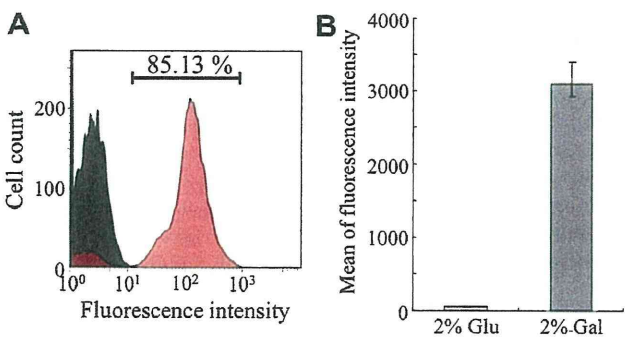

Fig.2. Induction of *GFP* reporter gene in the presence of galactose. To check induction of the *GFP* reporter gene by the *GAL1* promoter in the presence of galactose, the RIG-0 yeast strain, whose *GAL1* gene was replaced by the *GFP* gene, was incubated in SD medium (containing 2% glucose) or SG medium (containing 2% galactose) for 18 h. The GFP fluorescence of 10,000 cells was measured by flow cytometry. (A) Histogram plots of RIG-0 strain grown in SD medium (filled gray) and in SG medium (filled red). (B) Mean values of the green fluorescence signal of 10,000 cells. Error bars represent the standard deviations ($n = 3$). (For interpretation of the references to color in this figure legend, the reader is referred to the Web version of this article.)

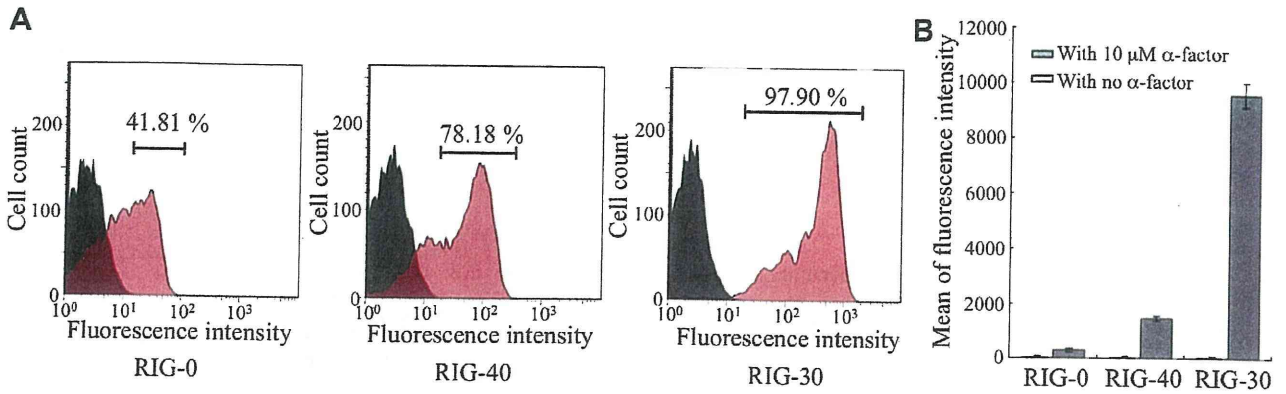

Fig.3. Effect of agonist-induced GPCR signaling on induction of the *GFP* reporter gene in GAL regulon transplanted yeast strains. The RIG-0 strain, whose *GAL1* gene was replaced by the *GFP* gene, was used as a control strain. Based on the RIG-0 strain, we generated the RIG-40 and RIG-30 strains that express the *GAL4* and *GAL3*^{c} genes, respectively, under the control of the pheromone-responsive *FIG1* promoter. All engineered strains were incubated in SDLG medium with or without 10 μM α-factor for 18 h. The GFP fluorescence of 10,000 cells was measured by a flow cytometer. (A) Histogram plots of RIG-0, RIG-40, and RIG-30 strains grown without α-factor (filled gray) and with 10 μM α-factor (filled red). (B) Mean values of the green fluorescence signal of 10,000 cells. Error bars represent the standard deviations ($n = 3$). (For interpretation of the references to color in this figure legend, the reader is referred to the Web version of this article.)

level of the *GFP* reporter gene by the *GAL1* promoter in the presence of galactose, the RIG-0 strain was cultivated in medium containing 2% glucose (without induction) or 2% galactose (with induction) as a carbon source. We then measured the GFP fluorescence level of each yeast cell by flow cytometry (Fig. 2A). As expected, the average fluorescence of RIG-0 was elevated in the presence of galactose, exhibiting a greater than 50-fold increase in fluorescence intensity compared with cultivation in the presence of glucose (Fig. 2B). Thus, in the RIG-0 strain, the galactose-mediated GAL regulatory machinery was able to induce the *GFP* reporter gene robustly under the control of the *GAL1* promoter.

To verify the validity of our concept, the *GAL4* or *GAL3*^{c} gene was substituted for the pheromone-responsive *FIG1* gene in the genome of RIG-0, yielding the RIG-40 or RIG-30 strain, respectively (Table 1). For activation of G-protein signaling, the engineered yeast strains were cultivated in galactose-free glycerol/lactate medium (containing marginal glucose of 0.05%) with or without 10 μM α-factor, and the fluorescence level of each yeast cell was measured by flow cytometry (Fig. 3). As expected, the introduction of the *GAL4* or *GAL3*^{c} gene into the pheromone-responsive gene locus of the RIG-0 strain induced GFP fluorescence downstream of GPCR stimulation (Fig. 3A). Surprisingly, the induction level of the *GFP* reporter gene in response to GPCR stimulation was higher than that by galactose (Fig. 2). The limited fluorescence of the RIG-0 negative control strain in the presence of α-factor probably reflected changes in intrinsic fluorescence invoked by signal activation (Fig. 3A). Whereas agonist stimulation increased GFP fluorescence in the RIG-40 strain approximately 25-fold, the RIG-30 displayed a greater than 150-fold increase in fluorescence intensity (Fig. 3B).

One possible explanation for this critical difference between pheromone-responsive GFP expression of the RIG-40 and RIG-30 yeast strains may be due largely to the effect of Gal80 (a Gal4 repressor), which promotes Gal4-mediated transcription by interacting with Gal3^{c}. Indeed, we observed that a yeast strain that lacks Gal80 (*gal80Δ*), with an integrated *GFP* reporter gene in the *GAL1* locus, produced a green fluorescent signal even in the absence of α-factor stimulation (data not shown). Briefly, Gal80 not bound to endogenous Gal4 might inhibit the activity of pheromone-induced overexpressed Gal4 because Gal4 is the direct transcriptional activator of the GAL regulon. However, the constitutively active Gal3 mutant, Gal3^{c}, is capable of activating the GAL regulon because it can inhibit the Gal80/Gal4 interaction despite the presence of endogenous Gal80 [22–25].

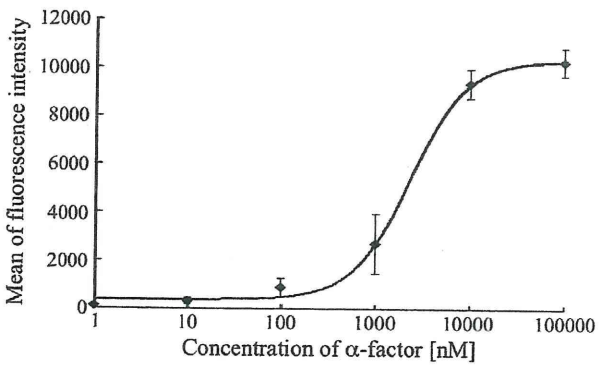

Fig.4. Dose–response curve for various concentrations of α-factor in GAL regulon engineered RIG-30 strain. The RIG-30 strain, whose *GAL1* gene and *FIG1* gene were replaced by the *GFP* and *GAL3*^{c} genes, respectively, was incubated in SDLG medium with indicated concentrations of α-factor for 18 h. The GFP fluorescence of 10,000 cells was measured by a flow cytometer. Mean values of the green fluorescence signal of 10,000 cells are shown. Error bars represent the standard deviations ($n = 3$).

In addition, we examined the data from our engineered yeast strains to test the assumption that our system could be applied for the screening of novel GPCR agonists by flow cytometry Ishii et al. [26] (Fig. 3A). Flow cytometry easily distinguished the agonist-stimulated RIG-30 yeast cells from the nonactivated cells, with a significant GFP signal detected in up to 98% of the cell population, supporting the possibility that our method could easily permit quantitative, high-throughput, flow cytometric screening of novel GPCR agonists.

Finally, we investigated whether we could use our system as a sensing tool for agonist-specific signaling. As shown in Fig. 4, the RIG-30 exhibited a dose-dependent increase in GFP fluorescence, the result of increasing α-factor concentration. Moreover, the half-maximal effective concentration (EC_{50}) was calculated to be 1.43 ± 0.27 μM. These results clearly show a significant and sensitive GFP reporter induction in RIG-30, the result of the GPCR ligand α-factor.

Conclusion

In this study, we successfully established a highly robust reporter gene assay system for detecting GPCR agonists by transplanting the GAL regulon into G-protein signaling circuitry in yeast. Our

system, designed to express the constitutively active Gal3 mutant ($Gal3^c$) under the control of the pheromone-responsive *FIG1* promoter, agonist stimulation achieved a greater than 150-fold increase in reporter intensity. In addition, flow cytometry screening could distinguish an agonist-induced signal in up to 98% of cells. Our method could be applied to the quantitative, high-throughput screening of novel GPCR agonists.

Acknowledgments

This work was supported by Special Coordination Funds for Promoting Science and Technology, Creation of Innovation Centers for Advanced Interdisciplinary Research Areas (Innovative Bioproduction Kobe, iBioK), MEXT, Japan, and funded in part by the Naito Foundation.

Appendix A. Supplementary data

Supplementary data associated with this article can be found, in the online version, at doi:10.1016/j.ab.2012.02.005.

References

[1] A. Traven, B. Jelicic, M. Sopta, Yeast Gal4: a transcriptional paradigm revisited, EMBO Rep. 7 (2006) 496–499.
[2] S.A. Ramsey, J.J. Smith, D. Orrell, M. Marelli, T.W. Petersen, P. de Atauri, H. Bolouri, J.D. Aitchison, Dual feedback loops in the GAL regulon suppress cellular heterogeneity in yeast, Nat. Genet. 38 (2006) 10082–10087.
[3] R. Yang, S.C. Lenaghan, J.P. Wikswo, M. Zhang, External control of the GAL network in *S. cerevisiae*: a view from control theory, PLoS One 6 (2011) 19353.
[4] O. Demir, I. Aksan Kurnaz, An integrated model of glucose and galactose metabolism regulated by the GAL genetic switch, Biol. Chem. 30 (2006) 179–192.
[5] C.Q. Diep, X. Tao, V. Pilauri, M. Losiewicz, T.E. Blank, J.E. Hopper, Genetic evidence for sites of interaction between the Gal3 and Gal80 proteins of the *Saccharomyces cerevisiae* GAL gene switch, Genetics 178 (2008) 725–736.
[6] J. Ishii, N. Fukuda, T. Tanaka, C. Ogino, A. Kondo, Protein–protein interactions and selection: yeast-based approaches that exploit guanine nucleotide-binding protein signaling, FEBS J. 277 (2010) 1982–1995.
[7] R. Heilker, M. Wolff, C.S. Tautermann, M. Bieler, G-protein-coupled receptor-focused drug discovery using a target class platform approach, Drug Discov. Today 14 (2009) 231–240.
[8] G.D. Stewart, C. Valant, S.J. Dowell, D. Mijaljica, R.J. Devenish, P.J. Scammells, P.M. Sexton, A. Christopoulos, Determination of adenosine A1 receptor agonist and antagonist pharmacology using *Saccharomyces cerevisiae*: implications for ligand screening and functional selectivity, J. Pharmacol. Exp. Ther. 331 (2009) 277–286.
[9] S.J. Dowell, A.J. Brown, Yeast assays for G-protein-coupled receptors, Receptors Channels 8 (2002) 343–352.
[10] Y. Iguchi, J. Ishii, H. Nakayama, A. Ishikura, K. Izawa, T. Tanaka, C. Ogino, A. Kondo, Control of signalling properties of human somatostatin receptor subtype-5 by additional signal sequences on its amino-terminus in yeast, J. Biochem. 147 (2010) 875–884.
[11] S. Togawa, J. Ishii, A. Ishikura, T. Tanaka, C. Ogino, A. Kondo, Importance of asparagine residues at positions 13 and 26 on the amino-terminal domain of human somatostatin receptor subtype-5 in signaling, J. Biochem. 147 (2010) 867–873.
[12] Y. Fukutani, T. Nakamura, M. Yorozu, J. Ishii, A. Kondo, M. Yohda, The N-terminal replacement of an olfactory receptor for the development of a yeast-based biomimetic odor sensor, Biotechnol. Bioeng. 109 (2012) 205–212.
[13] B.J. Evans, Z. Wang, J.R. Broach, S. Oishi, N. Fujii, S.C. Peiper, Expression of CXCR4, a G-protein-coupled receptor for CXCL12 in yeast identification of new-generation inverse agonists, Methods Enzymol. 460 (2009) 399–412.
[14] G. Ladds, A. Goddard, J. Davey, Functional analysis of heterologous GPCR signalling pathways in yeast, Trends Biotechnol. 23 (2005) 367–373.
[15] R. Panetta, Y. Guo, S. Magder, M.T. Greenwood, Regulators of G-protein signaling (RGS) 1 and 16 are induced in response to bacterial lipopolysaccharide and stimulate c-fos promoter expression, Biochem. Biophys. Res. Commun. 259 (1999) 550–556.
[16] C.Q. Diep, G. Peng, M. Bewley, V. Pilauri, I. Ropson, J.E. Hopper, Intragenic suppression of Gal3C interaction with Gal80 in the *Saccharomyces cerevisiae* GAL gene switch, Genetics 172 (2006) 77–87.
[17] D. Gietz, A. St. Jean, R.A. Woods, R.H. Schiestl, Improved method for high efficiency transformation of intact yeast cells, Nucleic Acids Res. 20 (1992) 1425.
[18] R. Akada, T. Kitagawa, S. Kaneko, D. Toyonaga, S. Ito, Y. Kakihara, H. Hoshida, S. Morimura, A. Kondo, K. Kida, PCR-mediated seamless gene deletion and marker recycling in *Saccharomyces cerevisiae*, Yeast 23 (2006) 399–405.
[19] C.B. Brachmann, A. Davies, G.J. Cost, E. Caputo, J. Li, P. Hieter, J.D. Boeke, Designer deletion strains derived from *Saccharomyces cerevisiae* S288C: a useful set of strains and plasmids for PCR-mediated gene disruption and other applications, Yeast 14 (1998) 115–132.
[20] E.A. Winzeler, D.D. Shoemaker, A. Astromoff, H. Liang, K. Anderson, B. Andre, R. Bangham, R. Benito, J.D. Boeke, H. Bussey, A.M. Chu, C. Connelly, K. Davis, F. Dietrich, S.W. Dow, M. El Bakkoury, F. Foury, S.H. Friend, E. Gentalen, G. Giaever, J.H. Hegemann, T. Jones, M. Laub, H. Liao, N. Liebundguth, D.J. Lockhart, A. Lucau-Danila, M. Lussier, N. M'Rabet, P. Menard, M. Mittmann, C. Pai, C. Rebischung, J.L. Revuelta, L. Riles, C.J. Roberts, P. Ross-MacDonald, B. Scherens, M. Snyder, S. Sookhai-Mahadeo, R.K. Storms, S. Véronneau, M. Voet, G. Volckaert, T.R. Ward, R. Wysocki, G.S. Yen, K. Yu, K. Zimmermann, P. Philippsen, M. Johnston, R.W. Davis, Functional characterization of the *S. cerevisiae* genome by gene deletion and parallel analysis, Science 285 (1995) 901–906.
[21] J. Ishii, T. Tanaka, S. Matsumura, K. Tatematsu, S. Kuroda, C. Ogino, H. Fukuda, A. Kondo, Yeast-based fluorescence reporter assay of G protein-coupled receptor signalling for flow cytometric screening: FAR1-disruption recovers loss of episomal plasmid caused by signalling in yeast, J. Biochem. 143 (2008) 667–674.
[22] M. Rubio-Texeira, A comparative analysis of the GAL genetic switch between not-so-distant cousins *Saccharomyces cerevisiae* versus *Kluyveromyces lactis*, FEMS Yeast Res. 5 (2005) 1115–1128.
[23] P.J. Bhat, T.V. Murthy, Transcriptional control of the GAL/MEL regulon of yeast *Saccharomyces cerevisiae:* mechanism of galactose-mediated signal transduction, Mol. Microbiol. 40 (2001) 1059–1066.
[24] O. Egriboz, F. Jiang, J.E. Hopper, The rapid GAL gene switch of *Saccharomyces cerevisiae* depends on nuclear Gal3, not nucleo-cytoplasmic trafficking of Gal3 and Gal80, Genetics 189 (2011) 825–836.
[25] R. Wightman, R. Bell, R.J. Reece, Localization and interaction of the proteins constituting the GAL genetic switch in *Saccharomyces cerevisiae*, Eukaryot. Cell 7 (2008) 2061–2068.
[26] J. Ishii, N. Yoshimoto, K. Tatematsu, S. Kuroda, C. Ogino, H. Fukuda, A. Kondo, Cell wall trapping of autocrine peptides for human G-protein-coupled receptors on the yeast cell surface, PLoS ONE, submitted for publication.

1944–1953 *Nucleic Acids Research, 2012, Vol. 40, No. 5*
doi:10.1093/nar/gkr979

Published online 10 November 2011

Functional and direct interaction between the RNA binding protein HuD and active Akt1

Toshinobu Fujiwara[1,*], Akira Fukao[2], Yumi Sasano[3], Hidenori Matsuzaki[4], Ushio Kikkawa[4], Hiroaki Imataka[5], Kunio Inoue[2], Shogo Endo[6], Nahum Sonenberg[7], Christian Thoma[8,*] and Hiroshi Sakamoto[2,*]

[1]Laboratory of Disease Biology, Institute of Microbial Chemistry, 3-14-23 Kamiosaki, Shinagawa-ku, Tokyo 141-0021, [2]Department of Biology, Graduate School of Science, Kobe University, [3]Research & Development Center, Nagase & Co., Ltd. 2-2-3 Murotani, Nishi-ku, Kobe, Hyogo 651-2241, [4]Biosignal Research Center Kobe University, 1-1 Rokkodaicho, Nada-ku, Kobe 657-8501, [5]Department of Materials Science and Chemistry, Graduate School of Engineering, University of Hyogo, Himeji 671-2280, [6]Aging Regulation Research Team, Tokyo Metropolitan Institute of Gerontology, Itabashi, Tokyo 173-0015, Japan, [7]Department of Biochemistry and McGill Cancer Centre, McGill University, Montreal, Quebec, H3G 1Y6, Canada and [8]Department of Medicine II, University Hospital of Freiburg, Hugstetterstr 55, 79106 Freiburg, Germany

Received June 29, 2011; Revised and Accepted October 14, 2011

ABSTRACT

The RNA binding protein HuD plays essential roles in neuronal development and plasticity. We have previously shown that HuD stimulates translation. Key for this enhancer function is the linker region and the poly(A) binding domain of HuD that are also critical for its function in neurite outgrowth. Here, we further explored the underlying molecular interactions and found that HuD but not the ubiquitously expressed HuR interacts directly with active Akt1. We identify that the linker region of HuD is required for this interaction. We also show by using chimeric mutants of HuD and HuR, which contain the reciprocal linker between RNA-binding domain 2 (RBD2) and RBD3, respectively, and by overexpressing a dominant negative mutant of Akt1 that the HuD–Akt1 interaction is functionally important, as it is required for the induction of neurite outgrowth in PC12 cells. These results suggest the model whereby RNA-bound HuD functions as an adapter to recruit Akt1 to trigger neurite outgrowth. These data might also help to explain how HuD enhances translation of mRNAs that encode proteins involved in neuronal development.

INTRODUCTION

RNA binding proteins (RBPs) are key mediators of post-transcriptional control mechanisms, including the control of mRNA translation (1,2). This cytoplasmic regulatory mechanism also plays crucial roles in neuronal development (2). Several RBPs are specifically expressed in neurons such as the neuronal Hu proteins, which are essential for proper neuronal development and plasticity (3). The neuronal Hu family consists of three members, HuB, HuC and HuD. Hu proteins contain three RNA-binding domains (RBDs) and a linker region between RBD2 and RBD3 (3). The biological functions of Hu proteins result from their ability to bind to target mRNAs. Hu proteins stabilize adenine/uridine-rich element (ARE)-containing transcripts by binding to AREs via RBD1 and RBD2 and also affect translation (3). We have recently shown that HuD upregulates cap- and poly(A)-dependent translation through a direct interaction with eukaryotic initiation factor 4A (eIF4A) via its linker region (4). This enhancer function also involves the poly(A) binding activity of HuD via RBD3 (4). Interestingly, the linker region and RBD3 are also crucial for the stimulatory effect of HuD on neurite outgrowth, revealing a posttranscriptional role in neuronal development and plasticity (4). However, the underlying molecular mechanism(s) and interactions are poorly understood. In

*To whom correspondence should be addressed. Tel:/Fax: +81 3 3441 5375; Email: tosinobu@bikaken.or.jp
Correspondence may also be addressed to Christian Thoma. Tel:/Fax: +49 761 27032770; Email: christian.thoma@uniklinik-freiburg.de
Correspondence may also be addressed to Hiroshi Sakamoto. Tel: +81 78 803 5796; Fax: +81 78 803 5720; Email: hsaka@kobe-u.ac.jp
Present address:
Hidenori Matsuzaki, Department of Hygiene Kawasaki Medical School, 577 Matsushima, Kurashiki, Okayama 701-0192, Japan.

The authors wish it to be known that, in their opinion, the first two authors should be regarded as joint First Authors

particular, little is known about the involved signaling components. The phosphatidylinositol 3-kinase (PI3K)/Akt1 pathway is one of the major signaling transduction cascades regulating translation (5). Activated PI3K leads to an activation of Akt1. Activated Akt1 regulates protein synthesis via mammalian Target Of Rapamycin (mTOR) by targeting ribosomal protein S6 and multiple initiation factors including the components of the eIF4F complex. Interestingly, Akt1 signaling is also involved in the neurite outgrowth mechanism induced by nerve growth factor (NGF) (6). Here, we report that RNA-bound HuD interacts specifically and directly with active Akt1 to induce neurite outgrowth. We identify the linker region between RBD2 and RBD3 as the binding domain and show that the HuD–Akt1 interaction is functionally relevant as it is required for HuD-triggered neurite outgrowth in PC12 cells.

MATERIALS AND METHODS

Plasmids

Plasmids encoding T7-tagged mouse HuD proteins and glutathione-S-transferase (GST)-HuD fusion proteins were described previously (7,8). To generate the chimeric constructs FLAG-HuR-DL and FLAG-HuD-RL, the HuD- or HuR-linker, respectively, was inserted into the pFLAG HuR and HuD constructs. pFLAG-Akt1 dn was generated from pFLAG-Akt1 by replacing Lys179, Thr308 and Ser473 with Ala, using the QuikChange Site-Directed Mutagenesis Kit (Stratagene) (9,10).

Recombinant proteins

Hu proteins expressed in *Escherichia coli* as GST-fusions were purified as described (7,8). Recombinant active and inactive Akt1 were purchased from Upstate (Millipore).

Purification of FLAG-Akt1 and FLAG-eIF4B

HeLa cells were transfected with the expression plasmid coding for FLAG-tagged Akt1 or FLAG-tagged eIF4B and cultured for 48 h at 37°C. The purification procedures were carried out on ice. The extract from HeLa cells (1×10^7 cells) was lysed in lysis buffer (20 mM Tris–HCl, pH 7.5 containing 1 mM EDTA, 1 mM EGTA, 10 mM 2-mercaptoethanol, 1% Triton X-100, 150 mM NaCl, 10 mM NaF, 1 mM Na3VO4 and 50 μg/ml phenylmethylsulfonylfluoride), treated with benzonase and centrifuged at 18 000*g* for 10 min. The supernatant was incubated with FLAG M2 affinity gel (Sigma) equilibrated with lysis buffer for 3 h. After washing resin, FLAG-Akt was eluted with 100 μl of elution buffer (20 mM Tris–HCl, 150 mM NaCl, 1 mM EGTA, 1 mM EDTA, 10 mM 2-mercaptoethanol, 50 μg/ml phenylmethylsulfonyl fluoride and 100 μg/ml 3× FLAG-peptide) (11).

Cell culture and transfection

PC12 and HeLa cells were cultured in Dulbecco's modified Eagle's medium (Gibco) supplemented with 10% fetal bovine serum and 5% horse serum (for PC12 cells) or 10% fetal bovine serum (for HeLa cells), respectively. Cells were transiently transfected using the Lipofectamine 2000 transfection reagent (Invitrogen).

Immunoprecipitation

HeLa cells that have been cotransfected with the constructs coding for T7-HuD or T7-GFP and FLAG-tagged Akt1 were lysed in TNE buffer (20 mM Tris–HCl, pH 7.5, 150 mM NaCl, 2 mM EDTA, 1% NP-40, 1 mM phenylmethylsulfonyl fluoride, 10 μg/ml aprotinin and 10 μg/ml leupeptin). The extracts were then used for immunoprecipitation. Anti-T7 monoclonal antibody (Novagen) or anti-FLAG polyclonal antibody (Sigma) was added to the extracts together with protein G–sepharose beads. Bound proteins were eluted with SDS–PAGE loading buffer and subjected to SDS–PAGE and western blotting using anti-T7 monoclonal antibody and anti-FLAG polyclonal antibody.

In vitro binding experiments

GST pull-down assays were performed in TNE buffer (composition see above) as described previously (8). Bound proteins were separated by SDS–PAGE. Immunoblotting (IB) was performed with anti-FLAG, anti-Akt1 polyclonal antibodies and anti-GST monoclonal antibody (Sigma).

Determination of neurite-inducing activity in PC12 cells

After transfection of PC12 cells with constructs coding for T7-tagged or FLAG-tagged proteins, cells were cultured for 3 days and immunostained with anti-T7 polyclonal antibody (Bethyl) and anti-α-tubulin monoclonal antibody (Sigma). To address the role of Akt1 on the neurite-inducing activity of HuD, PC12 cells were cotransfected with T7-HuD or HuR-DL and either Akt1 dn or wild-type Akt1 and incubated for 3 days at 37°C. Immunostaining was then performed with anti-T7 polyclonal antibody and anti-FLAG monoclonal antibody (Sigma). Alexa 488 anti-rabbit IgG and Alexa 546 anti-mouse IgG were used as secondary antibodies, 1:1000 dilution (Invitrogen). Confocal analysis was performed using a confocal laser-scanning microscope (Zeiss LSM5 Pascal).

GSK-3β protein kinase assay

The enzyme activity of Akt1 was assayed by measuring the incorporation of radioactivity from [γ-^{32}P] ATP to glycogen synthase kinase 3β (GSK-3β) fusion protein (cell signaling), a synthetic substrate specific to Akt. Active Akt1 (upstate) was incubated with purified GST-HuD, GST-HuR or GST. Next, poly(U) beads were added to the mixture and incubated for 120 min. The poly(U) beads were collected by centrifugation and washed three times with TNE buffer. Before the kinase assay, the collected precipitates were washed at 0–4°C with 20 mM Tris–HCl pH 7.5 containing 1 mM EDTA, 1 mM EGTA, 10 mM 2-mercaptoethanol, 150 mM NaCl and 50 μg/ml phenylmethylsulfonyl fluoride to remove NP-40. The reaction mixture (25 μl) containing 20 mM Tris–HCl, pH 7.5, 10 mM $MgCl_2$, 20 mM ATP, 15–50 kBq of [γ-^{32}P] ATP and 100 mg/ml GSK-3β fusion

protein was then added to the precipitates and incubated for 30 min at 30°C. After boiling in SDS sample buffer, phosphorylated proteins were separated by SDS–PAGE. The radioactivity of the GSK-3β fusion protein band was analyzed by Bio-imaging Analyzer BAS2500 (Fujix).

In vitro kinase reaction using GST-HuD, FLAG-eIF4B or MBP-FOXO4

GST-HuD, FLAG-eIF4B or maltose-binding protein (MBP)-FOXO4 (Forkhead box protein O4) were incubated with and without active Akt1 in 20 mM Tris–HCl, pH 7.5, 10 mM $MgCl_2$, 20 μM ATP and [γ-^{32}P] ATP at 30°C for 30 min. After boiling in SDS-sample buffer, proteins were separated by SDS–PAGE. ^{32}P-labeled proteins were visualized using Bio-imaging Analyzer, BAS2500(Fuji) after Coomassie Brilliant Blue (CBB) staining (12).

RESULTS

HuD directly interacts with active Akt1

To examine the mechanism of how HuD induces neurite outgrowth, we used PC12 cells, which are an established model system for studying neuronal differentiation (13,14). PC12 cells can be induced to form neurites by overexpression of HuD (15). Using this system, we have recently shown that the eIF4A- and poly(A)-binding domains of HuD contribute to its neurite-inducing activity (4). We have also shown that these activities are critical for stimulating cap-dependent translation. Here, we further investigated the underlying molecular interactions.

Activation of the mTOR pathway by PI3K-Akt signaling is key for stimulating translation. Akt signaling promotes growth and proliferation including NGF-mediated neurite outgrowth induction (6). We hypothesized that (i) Akt1 function might be critical for the neurite-inducing activity of HuD and (ii) Akt1 might directly interact with HuD to fulfill this function. To examine this possibility, we performed first immunoprecipitation assays using HeLa cell lysates expressing FLAG-tagged Akt1 and T7-tagged HuD or GFP (Figure 1). Indeed, HuD, but not the negative control GFP, copurifies with FLAG-Akt1 (Figure 1A, left panel) and vice versa Akt1 copurifies with T7-HuD, but not with the control T7-GFP (Figure 1A, right panel).

To further confirm the interaction between endogenous Akt1 and HuD, we performed immunoprecipitation assays using PC12 cell lysates expressing T7-tagged HuD or GFP (Figure 1B) and examined coprecipitation of endogenous Akt1 with T7-tagged HuD or GFP. We found that endogenous Akt1 coimmunoprecipitated with T7-HuD but not with T7-GFP (Figure 1B).

Next, we tested whether the interaction is direct and specific or mediated by bridging RNA. To that end, we performed GST pull-down assays using purified recombinant GST-HuD and FLAG-tagged Akt1, which has been purified via FLAG M2 affinity gel (see 'Materials and Methods' section for further details) from benzonase-treated HeLa extracts before the GST pull-down assays (Figure 2A). We have used the endonuclease benzonase because it works well also at low temperatures and degrades all forms of RNA importantly also poly(A) RNA which is not digested by RNAse A. We found that FLAG-Akt1 copurifies with GST-HuD but not with the negative control GST (Figure 2A). Thus, the interaction between Akt1 and HuD is direct and specific.

To test whether active (phosphorylated) or inactive Akt1 interacts with HuD, we used commercially available

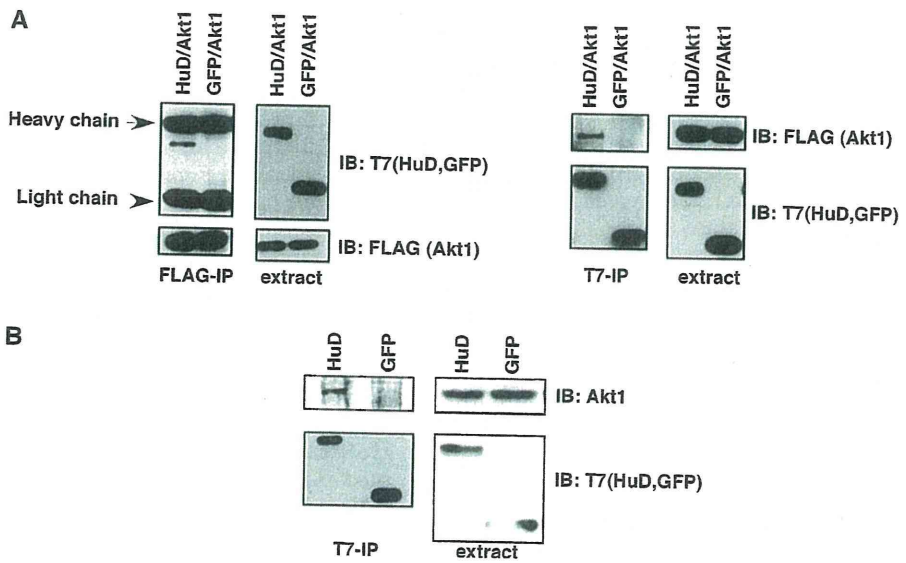

Figure 1. Protein–protein interaction by HuD and Akt1. (**A**) Specific coimmunoprecipitation of Akt1 with HuD. HeLa cells were transfected with T7-HuD or T7-GFP and FLAG-Akt1-coding plasmids. HuD was immunoprecipitated with anti-T7 antibody (right panel). Akt1 was immunoprecipitated with anti-FLAG antibody (left panel). Coimmunoprecipitation was monitored by IB. GFP is a negative control. (**B**) Specific coimmunoprecipitation of endogenous Akt1 with HuD. PC12 cells were transfected with T7-HuD- or T7-GFP-coding plasmids. HuD was immunoprecipitated with anti-T7 antibody. Coimmunoprecipitation of endogenous Akt1 was monitored by IB using anti-Akt1 antibodies.

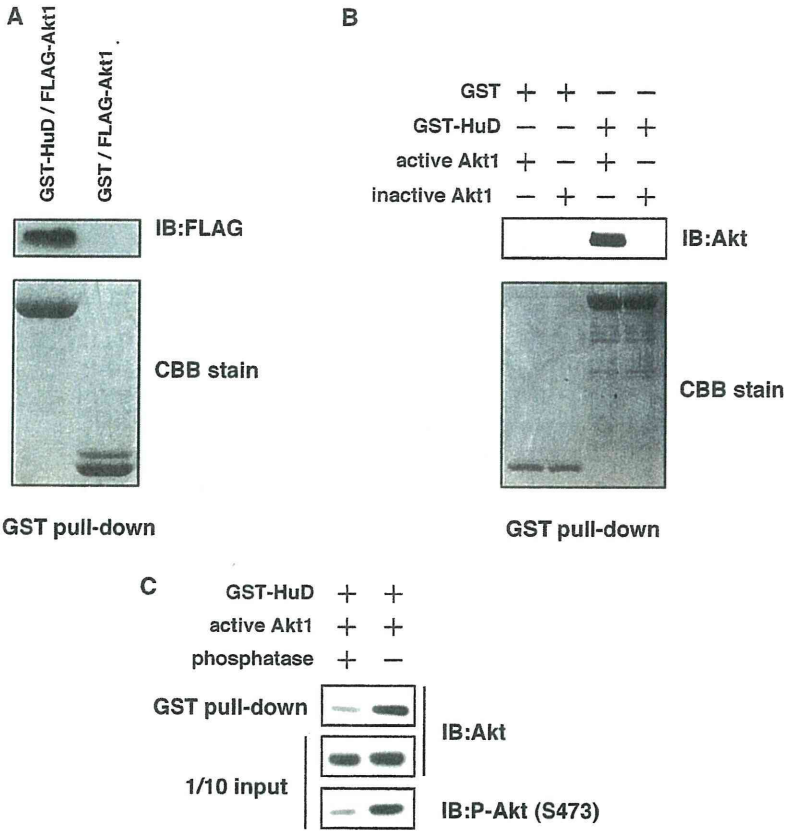

Figure 2. Direct protein–protein interaction by HuD and active Akt1. (**A**) RNA-independent interaction between HuD and Akt1. Purified FLAG-Akt1 derived from extracts treated with benzonase was incubated with GST-HuD or GST. GST pull-downs were examined for copurification of Akt1 by IB (upper panel) and for pull-down efficiency by CBB staining (lower panel). (**B**) and (**C**) RNA-independent interaction between HuD and active Akt1. Recombinant active or inactive Akt1 was incubated with GST-HuD or GST. (C) Active Akt1 and GST-HuD were incubated with or without lambda protein phosphatase, pulled down with glutathione-Sepharose beads and analyzed by IB (upper panel). One of 10 inputs was analyzed by IB for total and phospho-Akt1 levels (middle and lower panel of Figure 2C).

recombinant active and inactive Akt1 and performed GST pull-down assays using purified recombinant GST-HuD and active or inactive Akt1. Interestingly, we find that the phosphorylated form of Akt1 (active Akt1) interacts with HuD, as active, but not inactive Akt1 copurifies with GST-HuD (Figure 2B). To further confirm the interaction between HuD and active Akt1, we treated the samples with lambda protein phosphatase before the pull-down assays, which lead as expected to a strong reduction of phosphorylated Akt1 within the input samples and in line with the data shown above to a strong reduction of Akt1 in GST pull-down eluates (Figure 2C). Thus, we conclude that HuD binds directly and specifically to active/phosphorylated Akt1. In good agreement with these data, we also find that HuD colocalizes with active Akt1 in PC12 cells (Supplementary Figure S1).

Linker region of HuD is required for the interaction of HuD with Akt1

Next, we delineated the HuD sequence elements that are important for its interaction with Akt1 (Figure 3A). Using GST-HuD deletion mutants, we find that the linker region between amino acids 250 and 302 is required for the optimal interaction of HuD with Akt1 (Figure 3A). Interestingly, the overall amino acid sequence of Hu proteins is well conserved (4). However, the linker region of Hu proteins differs between the neuronal Hu proteins HuB, HuC and HuD and the ubiquitously expressed HuR (Supplementary Figure S2). HuR lacks a short sequence within the linker region, which is found in all neuronal Hu proteins (Supplementary Figure S2). This has prompted us to determine whether Akt1 interacts specifically with the neuronal Hu proteins but not with HuR. Indeed, Akt1 interacts with HuB, HuC and HuD but not with HuR (Figure 3B). To confirm the importance of the linker region in Akt1 binding, we generated chimeric mutants of HuD and HuR, which contain the reciprocal linker between RBD2 and RBD3, respectively (Figure 3C). As predicted, HuR carrying the HuD linker region gains the ability to bind Akt1 whereas HuD, containing the HuR linker regions looses its ability to interact with Akt1 (Figure 3C).

Role of Akt1 in HuD-induced neurite outgrowth in PC12 cells

We next wished to test whether the HuD–Akt1 interaction is functionally important. To address this question, we

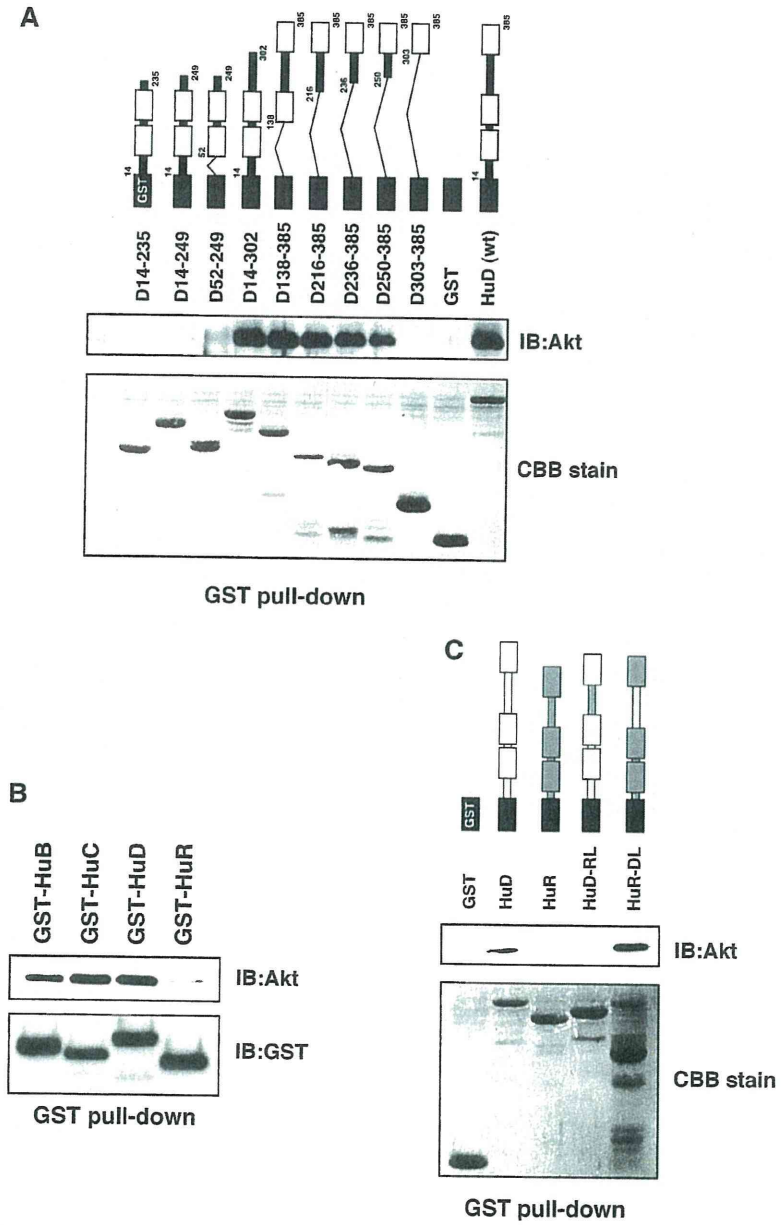

Figure 3. The linker region between RBD2 and RBD3 is required for HuD to interact with Akt1. (**A**) Akt1 was incubated with the indicated GST-HuD proteins. GST pull-downs were examined for copurification of Akt1 by IB (upper panel) and for pull-down efficiency by CBB staining (lower panel). The white rectangles represent the RBDs of HuD. (**B**) Akt1 specifically interacts with neuronal Hu proteins. Akt1 was incubated with the indicated proteins. (**C**) HuD binds Akt1 via the linker region of HuD. Akt1 was incubated with the indicated proteins.

used an established cell-based model system for studying neuronal differentiation, which is based on PC12 cells (13,14). If the HuD–Akt1 interaction is contributing significantly to the function of HuD, then our data predict that the chimeric HuR mutant should gain and the chimeric HuD mutant should loose its ability to induce neurite outgrowth. To test this prediction, we assayed the ability of the different HuD and HuR mutants described above to induce outgrowth in PC12 cells. As shown in Figure 4A and in concert with the data described above, wild-type HuD and the chimeric mutant HuR but not wild-type HuR or the chimeric HuD mutant transfected into PC12 cells can induce neurite outgrowth. These results suggest that binding of HuD to Akt1 is critical for the neurite-inducing activity of HuD. We note that wild-type HuD and the chimeric mutant HuR-DL that promotes neurite outgrowth are cytoplasmic, while those proteins that are not able to do so (wild-type HuR and the chimeric HuD mutant) are nuclear. To confirm that the Akt1 interaction with HuD and not just the cytoplasmic

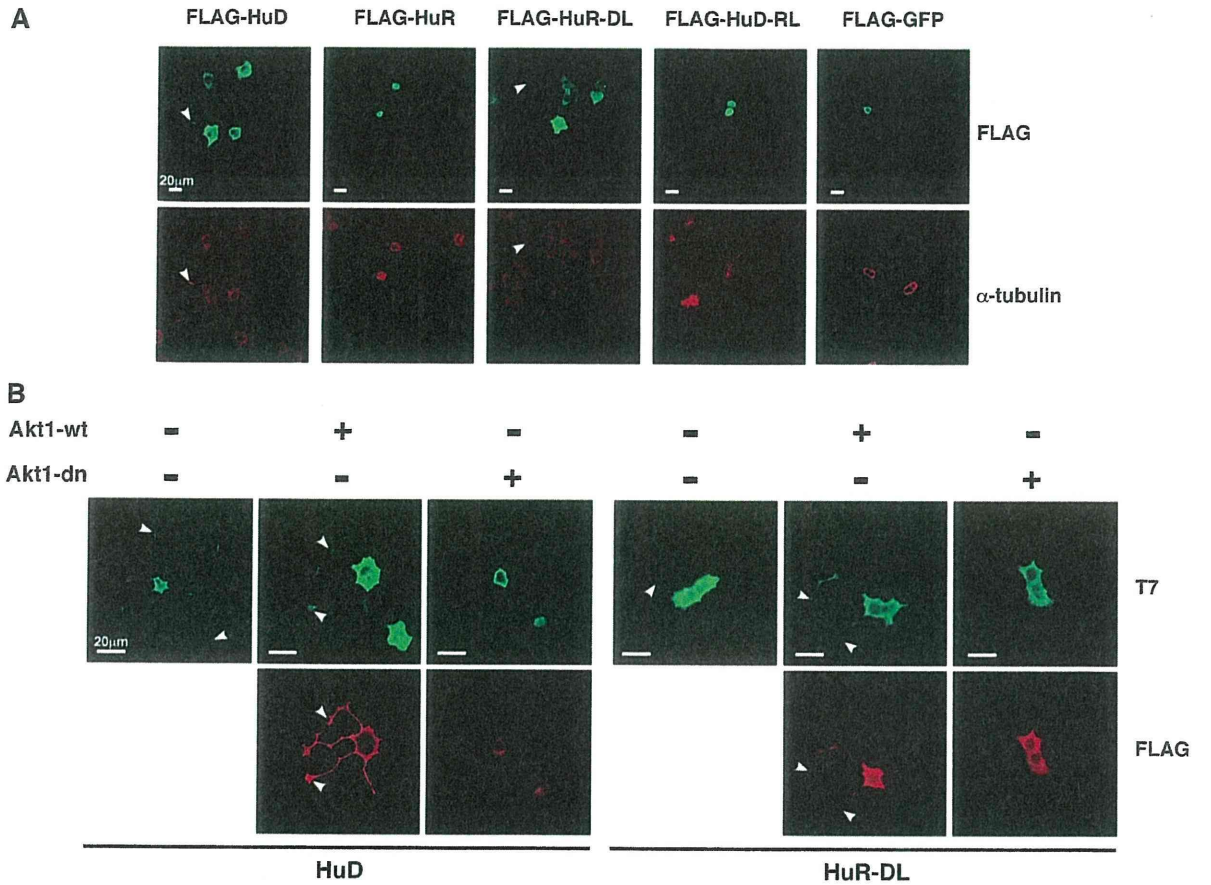

Figure 4. Role of the HuD–Akt1 interaction in neurite outgrowth. (**A**) Role of the linker region of HuD to induce neurite outgrowth. Shown is the confocal analysis of PC12 cells that have been transfected with constructs coding for the indicated proteins. Cells were costained with anti-FLAG (green) and with anti-α-tubulin antibody (red). Arrow heads point to induced neurites. Scale bar, 20 μm. The same results were obtained in at least three independent experiments. (**B**) Role of Akt1 in neuronal differentiation in PC12 cells induced by HuD and HuR-DL. Confocal analysis of PC12 cells that were transfected with constructs coding for the indicated proteins. Arrow heads point to induced neurites. Scale bar, 20 μm. The same results were obtained in at least three independent experiments.

location is the relevant component, we have further mapped linker region of HuD to identify the critical interaction domain. We find that the HuD mutant 277-385 containing a truncated linker region (277-302) and RBD3 is still capable of (i) interacting with Akt1 (Figure 5B) and (ii) inducing neurite outgrowth in PC12 cells (Figure 5C). Strikingly, we find that the truncated HuR mutant 219-327 containing an almost identical linker sequence (see scheme in Figure 5A for comparison) and RBD3 cannot interact with Akt1 (Figure 5B) and cannot induce outgrowth although it localizes to the cytoplasm (Figure 5C). Thus, we are confident to conclude that the interaction of HuD with Akt1 is the relevant component and not just the cytoplasmic localization.

To further test whether the induction of outgrowth correlates with Akt1 binding and function, we used a dominant negative mutant of Akt1 that is defective in ATP binding and has a phosphorylation site defect within the kinase domain (see 'Materials and Methods' section for further details). Binding of this inactive mutant to HuD is strongly reduced (Supplementary Figure S3). The results shown in Figure 4B further confirm the importance of Akt1 in HuD-induced neurite outgrowth as overexpression of dominant-negative Akt1 but not wild-type Akt1 inhibits neurite outgrowth induced by both HuD and the chimeric mutant HuR-DL.

RNA-bound HuD interacts with active Akt1

As all of the biological functions of HuD are believed to be a result of its ability to bind to RNA, we tested whether RNA-bound HuD can associate with Akt1. To address this question, we performed pull-down assays using poly(U) sepharose beads. Indeed, active but not inactive Akt1 associates with RNA-bound HuD (Figure 6A). This binding is specific, because it is not observed with GST or GST-HuR (Figure 6A). Importantly, active Akt1 associated with RNA-bound HuD retains its kinase activity (Figure 6B).

HuD itself is not the substrate for Akt1

We finally asked whether HuD is itself substrate for Akt1 phosphorylation or whether HuD recruits the kinase to a different substrate. To address this question, we have